RESEARCH ARTICLE

Triheptanoin Protects Motor Neurons and Delays the Onset of Motor Symptoms in a Mouse Model of Amyotrophic Lateral Sclerosis

Tesfaye W. Tefera[1☯], Yide Wong[1☯¤a], Mallory E. Barkl-Luke[1], Shyuan T. Ngo[1,2¤b], Nicola K. Thomas[1], Tanya S. McDonald[1], Karin Borges[1]*

1 School of Biomedical Sciences, The University of Queensland, Brisbane, Queensland, Australia,
2 University of Queensland Centre for Clinical Research, The University of Queensland, Brisbane, Queensland, Australia

☯ These authors contributed equally to this work.
¤a Current address: Queensland Institute of Medical Research, Brisbane, Queensland, Australia
¤b Current address: Queensland Brain Institute, The University of Queensland, Brisbane, Queensland, Australia
* k.borges@uq.edu.au

Abstract

There is increasing evidence that energy metabolism is disturbed in Amyotrophic Lateral Sclerosis (ALS) patients and animal models. Treatment with triheptanoin, the triglyceride of heptanoate, is a promising approach to provide alternative fuel to improve oxidative phosphorylation and aid ATP generation. Heptanoate can be metabolized to propionyl-CoA, which after carboxylation can produce succinyl-CoA and thereby re-fill the tricarboxylic acid (TCA) cycle (anaplerosis). Here we tested the hypothesis that treatment with triheptanoin prevents motor neuron loss and delays the onset of disease symptoms in female mice over-expressing the mutant human SOD1^{G93A} (hSOD1^{G93A}) gene. When oral triheptanoin (35% of caloric content) was initiated at P35, motor neuron loss at 70 days of age was attenuated by 33%. In untreated hSOD1^{G93A} mice, the loss of hind limb grip strength began at 16.7 weeks. Triheptanoin maintained hind limb grip strength for 2.8 weeks longer (p<0.01). Loss of balance on the rotarod and reduction of body weight were delayed by 13 and 11 days respectively (both p<0.01). Improved motor function occurred in parallel with alterations in the expression of genes associated with muscle metabolism. In gastrocnemius muscles, the mRNA levels of pyruvate, 2-oxoglutarate and succinate dehydrogenases and methylmalonyl mutase were reduced by 24–33% in 10 week old hSOD1^{G93A} mice when compared to wild-type mice, suggesting that TCA cycling in skeletal muscle may be slowed in this ALS mouse model at a stage when muscle strength is still normal. At 25 weeks of age, mRNA levels of succinate dehydrogenases, glutamic pyruvic transaminase 2 and the propionyl carboxylase β subunit were reduced by 69–84% in control, but not in triheptanoin treated hSOD1^{G93A} animals. Taken together, our results suggest that triheptanoin slows motor neuron loss and the onset of motor symptoms in ALS mice by improving TCA cycling.

Introduction

Amyotrophic Lateral Sclerosis (ALS) is a progressive neurodegenerative disorder characterized by selective degeneration of motor neurons in the brain and spinal cord that leads to muscle weakness, paralysis and death usually due to respiratory failure [1]. The typical age of onset for most forms of ALS is between 50 to 60 years and most patients die 3 to 5 years after symptom onset [2].

Ninety percent of ALS cases are sporadic (SALS), while 10% are familial (FALS) [3]. Mutations in genes such as superoxide dismutase 1 (*SOD1*) [4], TAR DNA-Binding Protein (*TDP 43*) [5], fused in sarcoma (*FUS*) [6], Ubiquilin2 (*UBQLN2*) [7], and *C9ORF72* [8,9] are implicated in genetic causes of ALS. Twenty percent of familial ALS cases are linked to mutations in the SOD1 gene (most commonly occurring mutation in patients with FALS) and this accounts for 1 to 2% of all forms of ALS while FUS and TDP-43 mutations account for 5% of FALS cases [3,10]. SOD1 mutations result in a toxic gain-of-function and are associated with misfolding and mislocalization of the SOD1 protein. While the normal SOD1 protein is usually found in the cytosol, mutant SOD1 accumulates within mitochondria and appears to contribute to many of the mitochondrial perturbations observed in ALS [11–15].

The exact mechanisms underlying selective motor neuron degeneration in ALS are unclear. The mechanisms causing motor neuron loss are multifactorial and may not be mutually exclusive [16]. Among many pathogenic mechanisms, major key pathological processes have been identified including oxidative stress [17], glutamate excitotoxicity [18], inflammation [19], abnormal protein aggregation [4,20], impaired axonal transport [21] and abnormalities in energy metabolism [22,23]. In addition, pathogenic processes in muscle seem to contribute to the progression of disease [24].

ALS and Energy Metabolism

Mitochondria are the main sites of energy production. The tricarboxylic acid (TCA) cycle together with the electron transport chain produce ATP, the primary cellular energy source that is necessary for cell function and survival. Functional and morphological abnormalities in mitochondria have been shown in the brain, spinal cord and muscles of patients with ALS and in mouse models of ALS [25–35]. Defects in mitochondrial respiration, the electron transport chain as well as ATP synthesis in the spinal cords of hSOD1^{G93A} mice [34], and reduced cellular ATP in the skeletal muscles and cerebral cortex of hSOD1^{G93A} mice have also been observed [36,37]. In this regard, impaired mitochondrial function in ALS is likely to underpin defective energy metabolism and a reduction in the capacity to produce ATP.

Reduced glucose metabolism has been shown in in various brain regions [38–42] and in the spinal cord [37,43] and muscles [36,44] of patients with ALS and mouse models of ALS. Indeed, the expression of several genes that encode for proteins and enzymes involved in glucose uptake, glycolysis, TCA cycle and the electron transport chain were found to be altered in fibroblasts cultured from ALS patients, in the motor cortex of ALS patients, and in the muscle and spinal cords of SOD1 mice [45–49]. Furthermore, there are indications that suggest reduction in levels of TCA cycle intermediates in SOD1 mouse brain and spinal cord and cellular models of ALS [50–52]. Collectively, these findings indicate that impaired ATP production, β-oxidation and TCA cycling contribute to metabolic aberrations in ALS.

Reduced levels of aspartate, glutamine and GABA in the spinal cord of hSOD1^{G93A} mice during early disease stages suggest that C4 intermediate levels of the TCA cycle are decreased [51]. In the CNS, glutamine supplies C4 carbons to glutamate and subsequently GABA and 2-oxoglutarate (α-ketoglutarate), while aspartate can be deaminated to form oxaloacetate (Fig 1). Low levels of oxaloacetate that can occur due to low supply of C4 TCA cycle intermediates and metabolites, including aspartate and glutamine, may impair the entry of acetyl-CoA
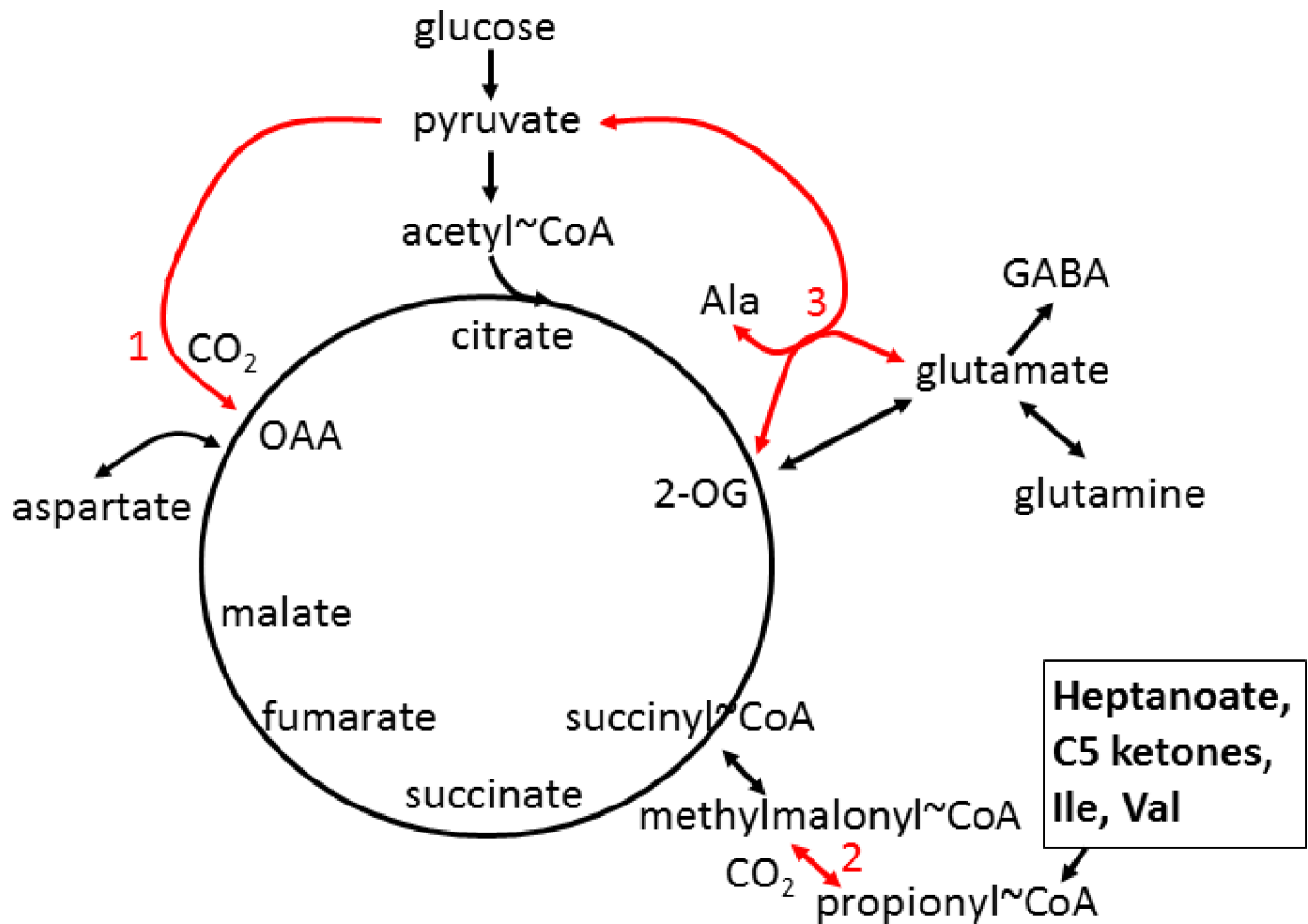
Fig 1. Simplified TCA cycle and anaplerosis in CNS and muscle. Red numbers indicate anaplerotic pathways, that can refill the levels of C4 intermediates of the cycle: **1** pyruvate carboxylase (mostly in CNS), **2** propionyl-CoA carboxylase, and **3** glutamic pyruvic transaminases (very important in muscle). C5 ketones, branched chain amino acids and heptanoate, are metabolized to propionyl-CoA and can therefore be anaplerotic via the propionyl-CoA carboxylation pathway. OAA–oxaloacetate, 2-OG– 2-oxoglutarate, Ile–isoleucine, Val—valine.

doi:10.1371/journal.pone.0161816.g001

generated from fuels into the TCA cycle. Therefore, the use of an alternative and additional fuel source that can "re-fill" the C4 carbon deficient TCA cycle intermediates (anaplerosis) may be of benefit in alleviating metabolic defects in ALS. When needed, anaplerosis is likely to improve ATP production in both the CNS and muscle especially during periods of energetic stress [53]. Thus, we suggest anaplerosis as a potential treatment approach for ALS.

Anaplerosis and Triheptanoin as a Treatment Approach

Anaplerosis serves to "re-fill" the levels of C4 carbon-deficient TCA cycle intermediates to improve energy supply during periods of increased energy need [53]. Anaplerotic enzymes include pyruvate carboxylase (*Pcx*), which produces oxaloacetate and glutamic pyruvic trans-aminases 1 and 2 (*Gpt1* and *2*), which catalyze the reaction pyruvate + glutamate $<=>$ α-ketoglutarate + alanine ([Fig 1]).

Triheptanoin, the triglyceride of heptanoic (C7) acid, not only provides an alternative fuel source in the form of medium chain fats, that are typically absent in a standard normal diet, but it can also be anaplerotic. It is a novel metabolic therapeutic that is being used in clinical

pilot studies to treat patients with various disorders associated with metabolic dysfunction. This includes genetic metabolic disorders of fatty acid oxidation [53,54] and neurological and muscular disorders [55–57]. Triheptanoin provides the body with heptanoate, which diffuses into the mitochondria of cells in both the CNS and peripheral tissues to be metabolized to acetyl-CoA and propionyl-CoA by β-oxidation. Also, the liver converts heptanoate into the "C5 ketones", β-hydroxypentanoate and β-ketopentanoate, which are then released into blood. After being taken up via monocarboxylate transporters into cells of various tissues, including the CNS, "C5 ketones" are also β-oxidized to acetyl-CoA and propionyl-CoA. Carboxylation of propionyl-CoA produces succinyl-CoA, a C4 TCA cycle intermediate via propionyl-CoA carboxylation, an anaplerotic pathway that has been described in various tissues [58–60] (Fig 1). An adequate supply of C4 TCA cycle intermediates is important for optimal oxidation of fuels by the TCA cycle [53,61].

There is now increasing evidence that triheptanoin improves energy metabolism in the CNS and muscle of patients and in animal models of different diseases, including brain and muscle in Huntington's Disease patients [55,62] and models of epilepsy [60,63]. Triheptanoin also was found to provide alternative fuel to the brains of patients and mice with glucose transporter 1 deficiency, which show impaired glucose uptake into the CNS [56,59]. In addition, there is evidence that triheptanoin can prevent cell loss in the brain in mouse models of stroke [64] and Canavan disease [65] by improving mitochondrial respiration.

Despite the beneficial effects observed following triheptanoin treatment in multiple models of disease and neurodegeneration, the use of triheptanoin as a potential therapeutic in ALS remains unexplored. Thus, we used hSOD1^{G93A} mice to test the hypotheses that 1) triheptanoin attenuates motor neuron death and delays the onset of motor symptoms, and that 2) the expression of enzymes involved in energy metabolism is diminished in muscle and can be rescued by triheptanoin.

Materials and Methods

Animals

All experiments were approved by the University of Queensland Animal Ethics Committee and followed the guidelines of the Queensland Animal Care and Protection Act 2001. Wild-type and hSOD1^{G93A} mice (B6.Cg-Tg(SOD1*G93A)1Gur/J, stock no. 004435, Jackson laboratory, Bar Harbor, ME, USA), were generated by mating hSOD1^{G93A} males with C57BL/6 wild-type females (University of Queensland). Mice were housed in a 12 hour light, 12 hour dark cycle, and had free access to food and water. Experimenters were blinded to animal genotype (until the mice started expressing the ALS phenotype) and treatment.

Triheptanoin Treatment

Starting at P35, female wild-type and hSOD1^{G93A} mice were given either control or triheptanoin-containing diet treatment until they were sacrificed. Untreated mice received SF11-027, a diet with ingredients typical to other mouse diets (Specialty Feeds, Glen Forrest, WA, AUS). Treated wild-type and hSOD1^{G93A} mice received a matched formulation (SF11-028, Specialty Feeds) in which 35% of the calories were from triheptanoin. This dose was chosen, as it is also used in the clinic to treat patients with metabolic disorders and has shown beneficial metabolic and protective effects in several animal models of various disorders [55,56,60,62–64,66]. The diets were matched in protein, mineral, antioxidant and vitamin content relative to their caloric densities [66]. Triheptanoin replaced sucrose, some of the complex carbohydrates and long chain fats. For the motor neuron count experiments, triheptanoin was provided by Ultragenyx Pharmaceutical Inc. (Novato, CA, USA). All other experiments were performed with triheptanoin obtained from Sasol GmbH (Germany).

Motor Neuron Counts

Mice were deeply anesthetized with pentobarbital (120 mg/Kg i.p. Provet, Northgate, QLD, AUS) and euthanized by decapitation. Spinal cords were flushed out of the spinal cavity using a cold phosphate buffered saline (PBS) filled syringe that was fitted with a blunted 23-gauge needle. Spinal cords were immediately fixed in 4% paraformaldehyde (PFA, pH 7.4) for 24 to 48 hours and then embedded in liquid paraffin. Serial, transverse sections (16μm) were obtained using a Leica Rotary Microtome. Motor neurons were identified after staining with thionine (0.1%) in acetate buffer (pH = 3.9). The L4 to L5 regions were identified according to standard anatomical guidelines described in [67] using an Olympus BX61 upright light microscope with 10x, 20x and 40x objectives. Briefly, the L4 and L5 sections were identified according to the area of the gracile fasciculus and dorsal corticospinal tract relative to the spinal cord central canal. In L3 sections, the dorsal corticospinal tract is smaller than in L4 and L5. Motor neuron numbers in L4 and L5 were determined using stereological principles based on the counting of every 10th section with a total of 11 to 16 sections counted [68]. Every tenth consecutive L4 and L5 spinal cord section was counted until the sacral dorsal commissural nucleus appeared concomitant with a decrease in size of the gracile fasciculus and dorsal corticospinal tract, which are markers for L6. Motor neurons were identified by a large, darkly stained cell body, a pale nucleus with a continuous boundary and one or more darkly stained nucleoli [67].

Blood ketone and glucose measurements

Blood plasma was collected in EDTA-coated tubes from the mice used for motor neuron counting, centrifuged at 2,000g for 10 mins. It was then stored at -80°C until analysis. Plasma levels of the ketone β-hydroxybutyrate and glucose were determined using Cayman colorimetric assay kits (Ann Arbor, MI, USA), according to the manufacturer's instructions.

Behavioral Testing and Observation

Animals underwent behavioral testing approximately 3–4 hours into the light cycle. All behavioral testing was conducted in an environment with minimal stimuli so as to minimize any possible effects caused by changes in external stimuli. Animals were weighed before every test session. Mice were observed, and disease progression tracked and graded according to a neurological score sheet [69] to ensure that any non-ALS related deaths were excluded from the study. In accordance with ethical requirements, hSOD1^{G93A} mice that became too weak to reach the food hoppers were provided with wet chow on the floor of the cages. The endpoint of the study was defined as the mouse being unable to right itself within 15 seconds after being placed on its back. Upon reaching end-stage or 25 weeks of age, transgenic mice and their respective wild-type littermates were euthanized with pentobarbital (120 mg/kg, i.p., Provet). Tissues, including the gastrocnemius muscle, were collected for subsequent analysis. To measure the time point when body weight loss started, we defined the day where a loss of more than 10% in an individual mouse occurred relative to its mean body weight from week 12 to 17. Also all subsequent three body weight measurements were $\leq$ 90% of the original mean weight.

Hind Limb Grip Strength Test

Hind limb grip strength tests were conducted twice a week using a T-bar force transducer (Ugo Basile, Varese, ITA). The animal was held by the tail, ensuring its hind limbs were gripping the T-bar before being pulled downwards at a 60° angle. The reading on the force transducer was taken only if both hind limbs released the bar at the same time. The average of 10 trials per

mouse was recorded for each training session [70]. To compare time points of grip strength loss, we determined the time point where a grip strength loss of more than 30% occurred in an inidividual mouse relative to its mean grip strength of week 9 to 13 and the subsequent three measurements were ≤ 70% of the original average strength.

Rotarod Test

Rotarod tests were conducted with 10 repeats once a week using a rotarod designed for mice (Ugo Basile). Animals were placed on the rod, which was then rotated for 3 min at 25 revolutions per minute [70]. The time at which the animal fell off was recorded. We defined the age of balance loss on the rotarod when this time was zero.

RNA Extraction, cDNA Synthesis, Quantitative Real Time PCR Assay

After euthanasia, the gastrocnemius muscle was quickly removed and frozen in liquid nitrogen. To extract RNA, muscle samples were pulverized in liquid nitrogen with a cold mortar and pestle, dissolved with TRI reagent (Life Technologies, Carlsbad, CA, USA) and extracted according to the manufacturer's instructions. Contaminating DNA was removed by DNAse I treatment and cDNA was synthesized using the Tetro cDNA synthesis kit (Bioline, London, UK) according to the manufacturer's instructions.

The expression of several metabolic genes was assayed (Table 1) by quantitative real time PCR.

All primer pairs were evaluated for efficiency using a 4 fold serial dilution series of muscle cDNA. The derived slope of each primer pair was used to calculate the efficiency by applying the formula, $4^{[(-1/slope)-1]*100}$. Reactions consisting of diluted cDNA, 5μl of SYBR Green master mix and 8μM of forward and reverse primers were amplified after an initial hot start. The thermal profile for the assay was an initial hot start of 95°C for 10 minutes, followed by 40 cycles of 95°C for 30 seconds, 60°C for 1 minute and 72°C for 30 seconds (ABI 7900HT Fast Real-Time PCR system, Applied Biosystems). Lastly the melt curve was generated by heating to 95°C for 2 minutes, cooling to 60°C for 15 seconds and a final 2% heating ramp to 95°C for 15 seconds. Samples without reverse transcriptase treatment were included to ensure that samples were free from DNA contamination. To select reference genes for normalization, expression of ten housekeeping genes in the different experimental groups were analyzed using GeNorm

Table 1. Gene names, symbol, forward and reverse primer sequences and of primers used for the gene expression studies of metabolic genes.

Gene	Symbol	Sequence 5' to 3'
β2-microglobulin	B2m	F AGACTGATACATACGCCTGCR ATCACATGTCTCGATCCCAG
Hydroxymethylbilane synthase	Hmbs	F AAGGGCTTTTCTGAGGCACCR AGTTGCCCATCTTTCATCACTG
TATA binding protein	Tbp	F TTCTCGAAAGAATTGCGCTGTR GCCTTGTGAGTCATTTCAGTG
Propionyl-CoA Carboxylase (Subunit α)	Pcca	F AGAATTGCAAGGGAAATTGG R CTAAAGCCATCCCTGGTCTC
Propionyl-CoA Carboxylase (Subunit β)	Pccb	F AGCCTACAACATGCTGGACA R GGTCCTCCCATTCATTCTTG
Methylmalonyl-CoA mutase	Mut	F CCAAACACTGACCGTTCTCA R GGAATGTTTAGCTGCTTCAGG
Pyruvate carboxylase	Pcx	F GAGCTTATCCCGAACATCCC R TCCATACCATTCTCTTTGGCC
Pyruvate dehydrogenase E1 α 1	Pdha1	F AACTTCTATGGAGGCAACGG R CTGACCCTGATTAGCAGCAC
Glyceraldehyde-3-phosphate dehydrogenase	Gapdh	F ATACGGCTACAGCAACAGGG R TCTTGCTCAGTGTCCTTGCT
Oxoglutarate dehydrogenase	Ogdh	F TGCAGATGTGCAATGATGAC R GCAGCACATGGAAGAAGTTG
Succinate dehydrogenase complex (Subunit A)	Sdha	F GGAACACTCCAAAAACAGACCT R CCACCACTGGGTATTGAGTAGAA
Glutamate-pyruvate transaminase 1	Gpt1	F TGAGGTTATCCGTGCCAATAR GTCCGGACTGCTCAGAAGAT
Glutamate-pyruvate transaminase 2 (alanine aminotransferase)	Gpt2	F GCGACGGTATTTCTACAATCCR CGCGGAGTACAAGGGATACT

doi:10.1371/journal.pone.0161816.t001

function. TATA binding protein (*Tbp*),β2-microglobulin (*B2m*) and Hydroxymethylbilane synthase (*Hmbs*) were chosen because they were the least changed in the experimental groups. The fold expression (ΔCT) of the gene of interest (goi) relative to the geometric mean of house-keeping genes (*Tbp*, *B2m* and *Hmbs*) were calculated with a formula adapted from [71] taking into consideration the individual efficiencies (E) of each primer pair.

$$\Delta CT_{goi} = 2^{-\left[(CT_{goi}Log_2 E_{goi}) - 3\sqrt{(CT_{TBP}Log_2 2.03)(CT_{B2m}Log_2 2.03)(CT_{HMBS}Log_2 1.86)}\right]}$$

Enzyme Assay

Mitochondrial extracts were prepared from the gastrocnemius muscle of male wild-type and hSOD1^{G93A} mice at different disease stages and homogenized with a glass-teflon homogenizer in 500 μL ice cold extraction buffer (0.32 M sucrose, 1 mM EDTA and 10 mM Tris-HCl, pH 7.4). Samples were centrifuged at 1000 g for 10 min at 4°C and the supernatant was then centrifuged at 12,000 g for 15 min at 4°C. The pellet was washed in 500 μL extraction buffer followed by another centrifugation at 12,000g for 15 min and then resuspended in cold extraction buffer with 0.1% Triton X-100. The ratio of buffer to tissue was 2.5 mL/g.

The maximal activities of 2-oxoglutarate dehydrogenase in these enriched mitochondrial extracts were determined via the reduction of nicotinamide adenine dinucleotide (β-NAD$^+$) in buffer (75 mM Tris HCl (pH 8), 1 mM ethylenediaminetetraacetic acid, 0.5 mM thiamine pyrophosphate, 1.5 mM Coenzyme A, 4 mM β-NAD$^+$, 1mM DTT, 2 mM calcium chloride) initiated with 15 mM 2-oxoglutarate, with background activity measured when no substrate was added [72]. The rate of NAD$^+$ reduction was measured with a spectrophotometric plate reader (Tecan, Mannedorf, CH), background activity was subtracted and the resultant activity was normalized to protein content measured with a Pierce Bicinchoninic acid assay (Thermo-Fisher Scientific, Scoresby, VIC, AUS). The amount of protein used was 10 μg per well.

Data Analysis

Statistical analyses were performed with Graphpad Prism (versions 5.03 and 6.0) using two-way ANOVAs followed by Bonferroni multiple comparisons post-hoc tests for analysis of several groups. For the comparison of the onset of body weight loss and the area under the curve (AUC) for hind limb grip strength, two-tailed unpaired t-tests were employed. Data are represented as mean ± SEM. Using the variation of our motor neuron numbers in our colony determined in a preliminary experiment, power analysis showed that to be able to observe a treatment effect of 30% with α = 0.05 and β = 80%, n = 8–9 mice were necessary, an sample size which is higher than in the guidelines [73]. In addition, power analysis using the average standard deviations for the onset of loss of grip strength and balance on rotarod showed that n = 5 was sufficient to observe changes between means by 2.3 and 1.5 weeks respectively with 80% power at the 0.05 significance level. We are aware that our study was underpowered for survival analyses based on the guidelines for preclinical ALS research [73].

Results

Triheptanoin Protected Against Motor Neuron Loss in hSOD1^{G93A} Mice

A defining hallmark of ALS is progressive motor neuron loss. Here, we confirmed that relative to wild-type mice, 38% of lumbar L4-L5 motor neurons were lost by 70 days of age in hSOD1^{G93A} mice (Fig 2, two-way ANOVA p<0.0001 for genotype, Bonferroni multiple

comparisons post hoc test p<0.0001, n = 7–10 per group). To determine if triheptanoin can protect motor neurons, we initiated triheptanoin treatment at P35 in female hSOD1[G93A] mice at 35% of caloric intake until P70. This dose was chosen, as it is also used in the clinic to treat patients with metabolic disorders and has shown beneficial metabolic and protective effects in several animal models of various disorders [55,56,60,62–64,66]. Starting triheptanoin treatment at P35 in hSOD1[G93A] mice resulted in higher motor neuron numbers by 18% relative to untreated hSOD1[G93A] mice (two-way ANOVA p = 0.0126 for treatment, Bonferroni multiple comparisons post hoc test p<0.05), amounting to a 33% protection against motor neuron loss.

Triheptanoin Delayed the Onset of the Loss of Hind Limb Grip Strength and Balance in hSOD1[G93A] Mice

We investigated the extent to which triheptanoin delays the onset of the progressive loss of muscle strength in hSOD1[G93A] mice. Hind limb grip strength tests were used to assess the
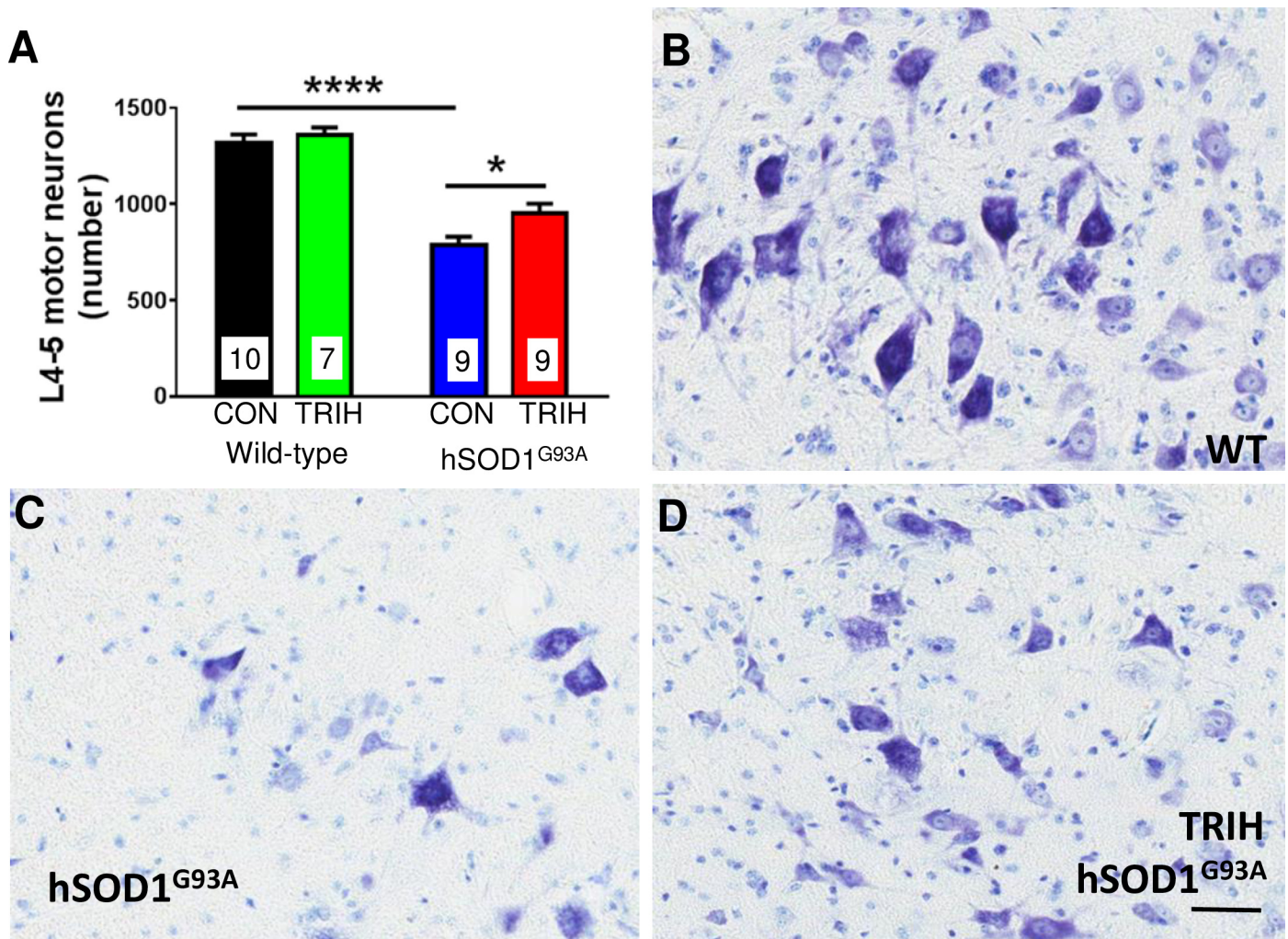

Fig 2. Triheptanoin preserves motor neurons. Starting at P35, female wild-type and hSOD1[G93A] mice were either treated with triheptanoin (TRIH) or control (CON) diet until P70. (A) Stereologically counted motor neuron numbers in the L4-L5 segments of these 70 day old mice (n = 7–10) revealed a 38% loss of motor neurons in control-fed hSOD1[G93A] mice. Triheptanoin provided a 33% protection against motor neuron loss. Two way ANOVA p<0.0001 for genotype, p = 0.0126 for treatment, the stars indicate results from a Bonferroni multiple comparisons post hoc tests if significant (**** p<0.0001, * p<0.05) (B-D) Representative thionine stained spinal cord sections from an untreated wild-type mouse (B) and untreated (C) and triheptanoin-treated (D) hSOD1[G93A] mice with arrows pointing to the motor neurons counted. Scale bar 100 µm.
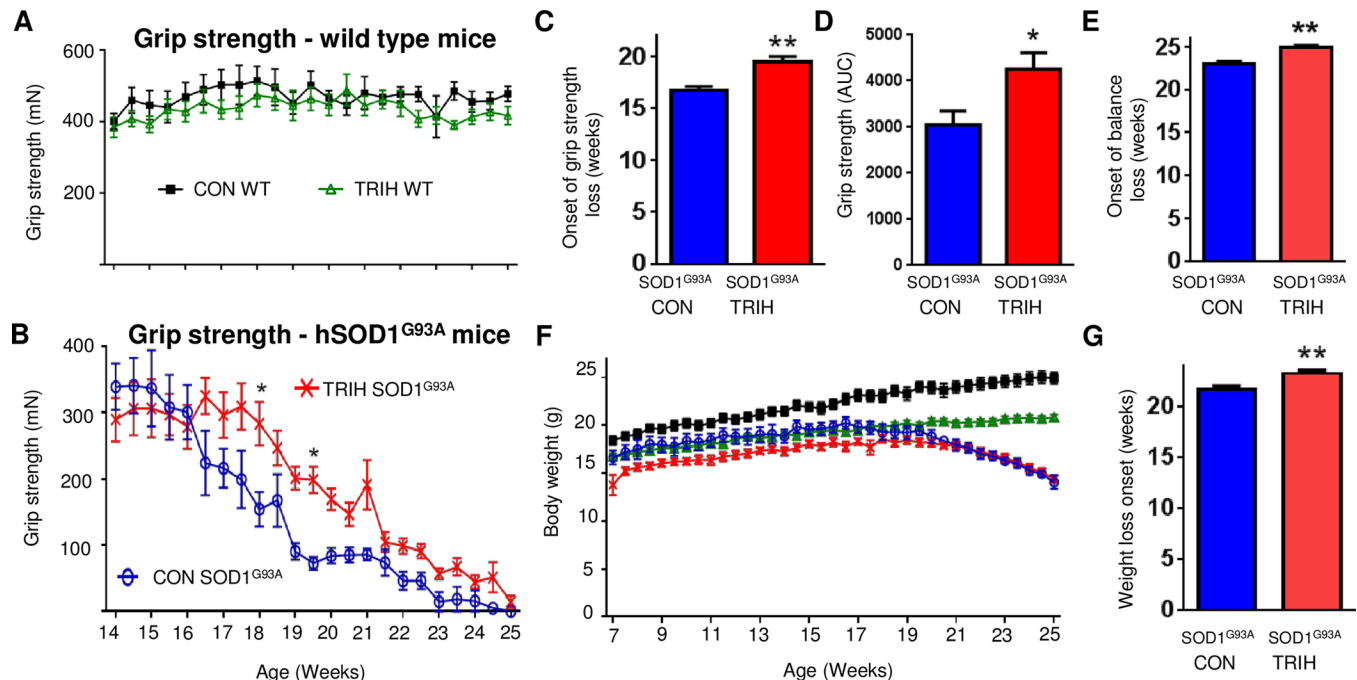
doi:10.1371/journal.pone.0161816.g002

Fig 3. Triheptanoin treatment delays the loss of hind limb grip strength in hSOD1^G93A mice. Starting at P35, female wild-type and hSOD1^G93A mice were treated with triheptanoin (TRIH) or control (CON) diet until they were sacrificed. (A) No differences in grip strength was observed between triheptanoin (green open triangles, n = 15) and control treated wild-type mice (black filled squares, n = 12). (B) The grip strength over time differed in triheptanoin treated (red crosses, n = 8) vs. untreated (blue empty circles, n = 5) hSOD1^G93A mice (p = 0.04, two way ANOVA), with treated mice having higher grip strength at 18 and 19.5 weeks (p<0.05 Bonferroni post-hoc test). (C) The onset of hind limb grip strength loss was delayed by 2.8 weeks in triheptanoin treated hSOD1^G93A mice when compared to untreated hSOD1^G93A mice (p = 0.002, t-test). (D) Overall hind limb grip strength shown as the area under the curve over time was increased in triheptanoin treated hSOD1^G93A mice compared to control treated hSOD1^G93A mice (p = 0.02, t-test). (E) The onset of balance loss in triheptanoin treated hSOD1^G93A mice was significantly delayed by 13 days (p = 0.0016, t-test). (F) Body weights over time were significantly different between triheptanoin treated vs. untreated wild-type mice and treated vs. untreated hSOD1^G93A mice. (G) The onset of body weight loss in triheptanoin treated vs. untreated hSOD1^G93A mice (n = 5) was delayed (p = 0.007, t-test). * p<0.05, ** p<0.01. The onset of body weight loss was defined as the day where a loss of more than 10% in an individual mouse occurred relative to the mean body weight from week 12 to 17 was observed. Also all subsequent three body weight measurements were ≤ 90% of the original mean weight.

course of disease progression in treated vs. untreated mice. There was no observable difference between the mean hind limb grip strength of the treated (n = 15) vs. untreated (n = 12) wild-type mice. Mean hind limb grip strength for both groups of wild-type mice consistently fell between 300 and 600 mN (Fig 3A). The hind limb grip strength of hSOD1^G93A mice on both treatments never exceeded 400 mN (Fig 3B). The time at which reduced hind limb grip strength became apparent was significantly later in triheptanoin treated hSOD1^G93A mice when compared to untreated hSOD1^G93A mice (n = 8 for triheptanoin treated, n = 5 for untreated mice; Fig 3B, p = 0.04, two way ANOVA). Bonferroni's multiple comparisons tests indicated that at 18 and 19.5 weeks of age, triheptanoin treated hSOD1^G93A mice had higher hind limb grip strength when compared to untreated hSOD1^G93A mice (Fig 3B, p<0.05). Untreated hSOD1^G93A mice began to lose hind limb grip strength at 16.7 weeks of age, but the time of onset of the loss of hind limb grip strength was delayed by 2.8 weeks in hSOD1^G93A mice that received oral triheptanoin (p = 0.002, Fig 3C). The area under the curve for the grip strength over time for each mouse treated with triheptanoin was increased by 38% (p = 0.024, t-test, Fig 3D).

In the rotarod test, behavior of the hSOD1^G93A mice varied widely. Many mice seemed "unmotivated" to perform on the rotating rod and no satisfying rotarod baseline performance was reached. Therefore we could only assess the time point when mice were unable to stay on

the rod. Triheptanoin treatment delayed the time of onset of loss of balance on the rod by 13 days (p = 0.0016; Fig 3E).

Body Weight Loss and Survival in hSOD1^{G93A} Mice with and without Triheptanoin

Body weight is another indicator of disease progression in hSOD1^{G93A} mice. When compared to untreated wild-type mice (n = 12), wild-type mice on oral triheptanoin (n = 15) gained weight at a slower rate (p<0.0001, Fig 3F). At 14 weeks of age, triheptanoin treated wild-type mice were approximately 3g lighter than untreated wild-type mice (p<0.05). This weight difference increased to approximately 4g at 22 weeks of age.

Both treated and untreated hSOD1^{G93A} mice (n = 5–8) were lighter when compared to untreated wild-type mice (p<0.0001). There were no differences in weight between hSOD1^{G93A} mice with or without triheptanoin treatment over the full time period. However, compared to control diet, triheptanoin fed hSOD1^{G93A} mice showed a trend of reduced body weight gain from 7–16 weeks. After 20 weeks of age, the body weight of hSOD1^{G93A} mice on the control and triheptanoin diet became similar (Fig 3F). The onset of body weight loss in hSOD1^{G93A} mice was delayed by 1.6 weeks (11 days) in triheptanoin treated mice (Fig 3G, p = 0.007, unpaired two-tailed t-test).

Based on power analysis and the guidelines for ALS research [73], this study of motor symptoms was too small to assess survival with adequate power. No differences were seen in the number of days taken to reach end-stage when comparing triheptanoin treated (n = 7) to untreated (n = 5) hSOD1^{G93A} mice (174.9±3.5 vs. 172.4±3.9, p = 0.653), indicating that in this small study, triheptanoin treatment did not alter survival.

Expression and Enzyme Activity Studies

Given the effect of triheptanoin on motor function in hSOD1^{G93A} mice, we next aimed to evaluate the extent to which TCA cycle metabolism or anaplerosis may be impaired in the gastrocnemius muscle of hSOD1^{G93A} mice in the early and late stages of the disease. We used quantitative real time PCR to compare the expression of genes encoding for enzymes involved in glycolysis (glyceraldehyde-3-phosphate dehydrogenase—*Gapdh*), the TCA cycle (pyruvate–*Pdha1*, 2-oxoglutarate—*Ogdh* and succinate dehydrogenases—*Sdha*, Fig 4) and anaplerotic pathways of the muscle. The latter include pyruvate carboxylase (*Pcx*) producing oxaloacetate, glutamic pyruvic transaminase 1 and 2 (*Gpt1* and *2*, Fig 5), and the enzymes of the propionyl-CoA carboxylation pathway (Fig 6), namely the α and β subunits of propionyl-carboxylase (*Pcca* and *Pccb*) and methylmalonyl mutase (*Mut*), which together metabolize propionyl-CoA to succinyl-CoA. Triheptanoin treated mice were included in this analysis to investigate the effect of triheptanoin on the expression of these metabolic enzymes.

Investigating the effects of genotype and treatment on the expression of key metabolic enzymes, two way ANOVAs revealed that the genotype was linked to the variations observed in the expression of several enzymes relative to housekeeping genes at 10 and/or 25 weeks of age (p shown in insets of bar graphs, Figs 4–6, n = 4–6). When compared to wild-type mice, 10 week old hSOD1^{G93A} mice showed a reduction in the expression of several dehydrogenases and methyl-malonyl mutase; namely the mRNA levels of the A1 subunit of pyruvate dehydrogenase (*Pdha1*) were reduced by 24%, 2-oxoglutarate dehydrogenase (*Ogdh*) by 30%, the subunit A of succinate dehydrogenase (*Sdha*) by 23%, and methyl-malonyl mutase (*Mut*) by 27.5% in hSOD1^{G93A} mice (Figs 4 and 6; all p<0.05 in Bonferroni post-test, n = 4–6 mice per group). Triheptanoin attenuated the reduction in the expression of pyruvate and succinate dehydrogenases in hSOD1^{G93A} mice. However, triheptanoin had no effect on the expression of
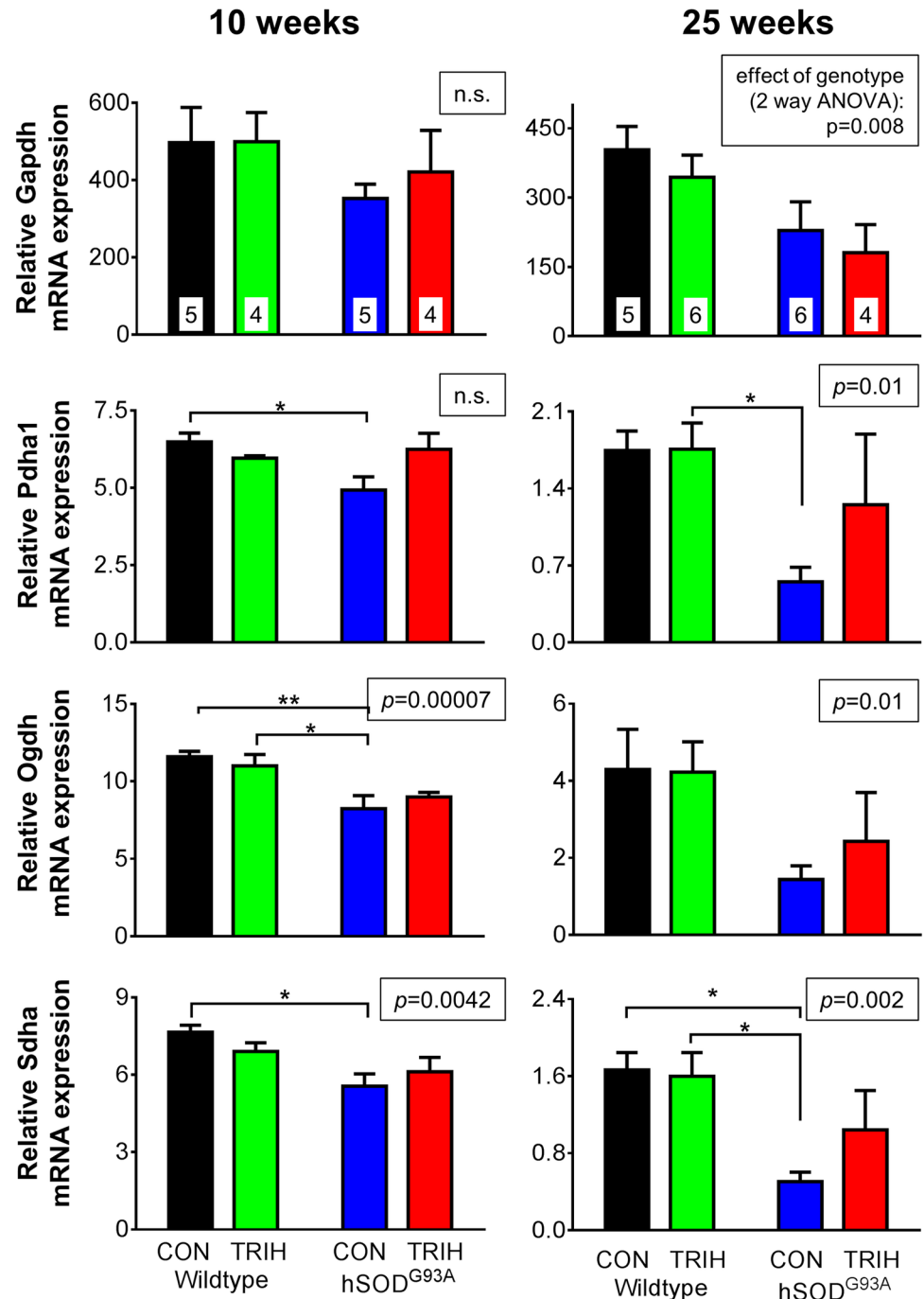
Fig 4. *Gapdh*, *Pdha*, *Ogdh* and *Sdha* mRNA expression in gastrocnemius muscle after triheptanoin treatment. Starting at P35, female wild-type and hSOD1[G93A] mice were treated with triheptanoin (TRIH) or control (CON) diet until they were sacrificed. Quantitative real time PCR analysis of *Gapdh*, *Pdha1*, *Ogdh* and *Sdha* of the gastrocnemius muscle of 10 and 25 week old wild-type and hSOD1[G93A] mice untreated or treated with triheptanoin relative to house keeping genes. N-numbers of each group used in all graphs are indicated in the top bar graphs. The insets above each graph show the p-values for the effects of genotype in two-way ANOVAs, while the effect of diet was p>0.05 for each bar graph. When significant, the results of Bonferroni post tests are shown by stars (* p<0.05, ** p<0.01), showing that decreases of mRNA levels of several enzymes in hSOD1[G93A] mice were not apparent with triheptanoin treatment.
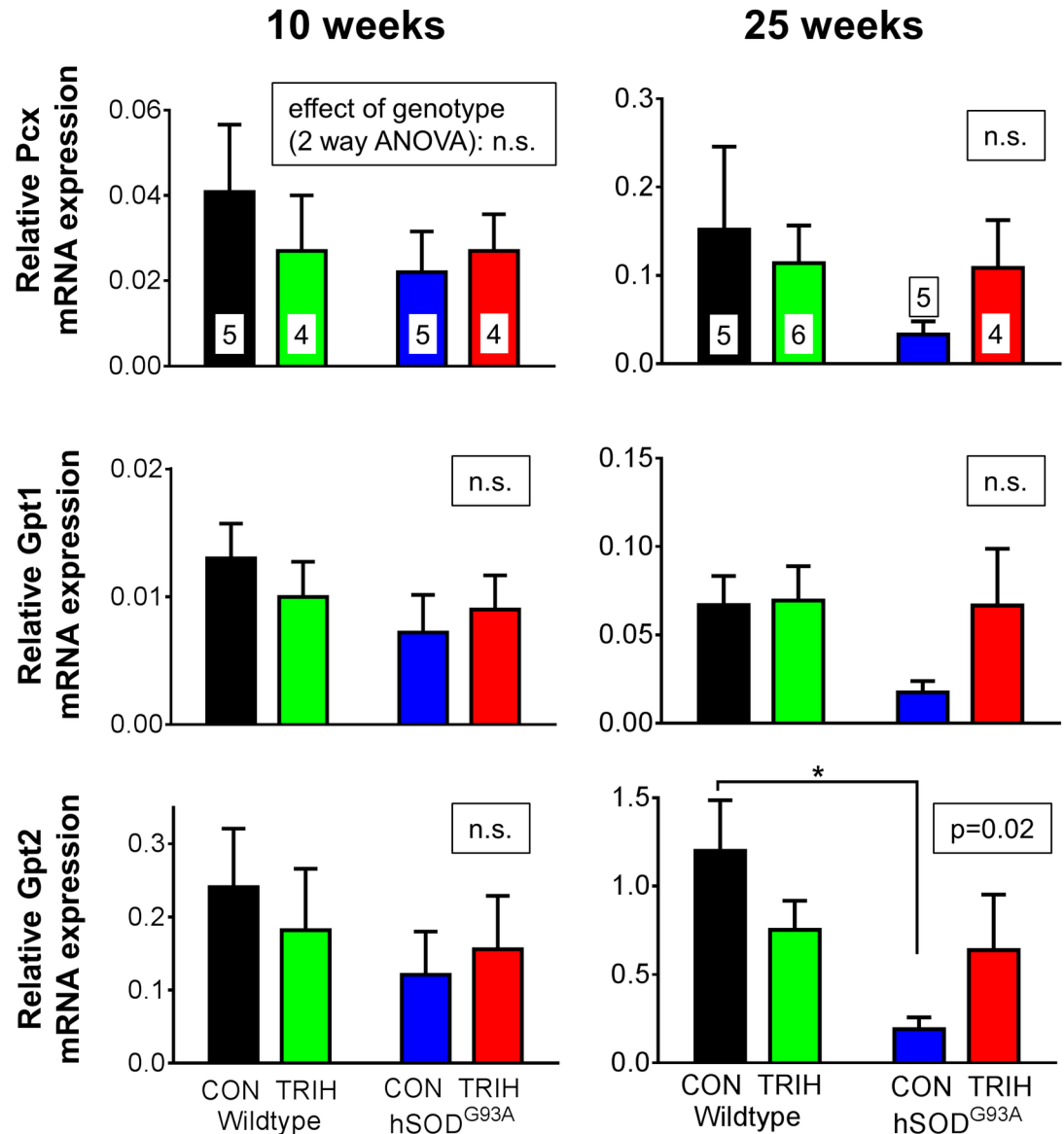
doi:10.1371/journal.pone.0161816.g004

Fig 5. Relative expression of the anaplerotic genes, pyruvate carboxylase *Pcx* and glutamic pyruvic transferases *Gpt1* and *2*. Starting at P35, female wild-type and hSOD1^{G93A} mice were either treated with triheptanoin (TRIH) or control (CON) diet until they were sacrificed. Gene expresssion is compared in the gastrocnemius muscle of 10 and 25 week old triheptanoin treated vs. untreated wild-type and hSOD1^{G93A} mice relative to housekeeping genes. N-numbers of each group used in all graphs are indicated in the top bar graphs. The insets above each graph show the p-values for the effects of genotype in two-way ANOVAs, while the effect of diet was p>0.05 for each bar graph. When significant, the results of Bonferroni post tests are shown by a star (* p<0.05), indicating that triheptanoin treatment prevented the decrease of expression in *Gpt2* mRNA.

doi:10.1371/journal.pone.0161816.g005

2-oxoglutarate dehydrogenase and methylmalonyl mutase. No alterations of mRNA levels were evident in the other investigated genes, including glycolytic *Gapdh* and the genes involved in anaplerosis, *Pcx*, *Gpt1* and *2*, *Pcca* and *Pccb* (Figs 4–6).

At 25 weeks of age, the end-stage of disease [67,74], and relative to untreated wild-type mice, hSOD1^{G93A} mice showed reduced gene expression for succinate dehydrogenase (*Sdha*, 70%), *Gpt2* (84%) and the β subunit of propionyl carboxylase (*Pccb*, 64%) (all p<0.05 in post
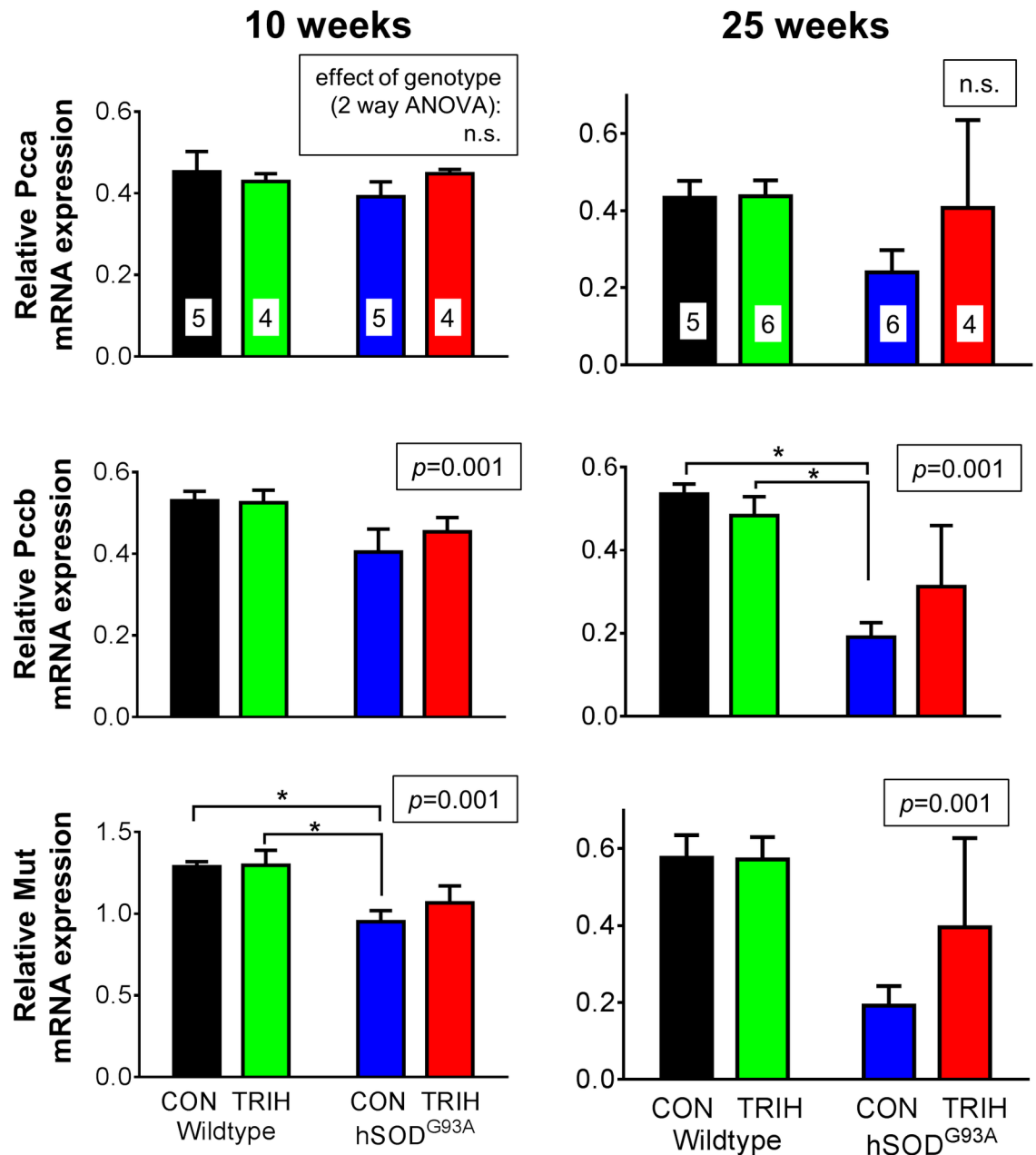
Fig 6. Gene expression of enzymes involved in the propionyl-CoA carboxylase pathway. Starting at P35, female wild-type and hSOD1[G93A] mice were treated with triheptanoin (TRIH) or control (CON) diet until they were sacrificed. Relative expression of the α (*Pcca*) and β (*Pccb*) subunits of propionyl-CoA carboxylase and methylmalonyl mutase (*Mut*). Expresssion is compared in the gastrocnemius muscle of 10 and 25 week old wild-type and hSOD1[G93A] mice untreated or treated with triheptanoin relative to housekeeping genes. N-numbers used for each group throughout the experiments are indicated in the top bar graphs. The insets above each graph show the p-values for the effects of genotype in two-way ANOVAs, while the effect of diet was p>0.05 for each bar graph. When significant, the results of Bonferroni post tests are indicated by a star (* p<0.05), indicating that triheptanoin treatment in hSOD1[G93A] mice protected against lowered expression of *Pccb* and *Mut* mRNA.

doi:10.1371/journal.pone.0161816.g006

test, Figs 4–6). Triheptanoin prevented the reduction in the expression of these genes, indicating that it can preserve muscle energy metabolism.

To investigate the extent to which these mRNA changes result in functional changes, we measured the maximal enzyme activity of 2-oxoglutarate dehydrogenase in extracts of gastrocnemius muscle in hSOD1^{G93A} compared to wild-type mice at different stages of disease (n = 4–6 mice each group). The two-way ANOVA analysis revealed that the maximal activity of this enzyme was significantly altered dependent on genotype (p<0.028) and disease stage (p<0.0007). At mid-stage (P110-130), there was a trend of a reduction by 25%, while the 45% loss of maximal 2-oxoglutarate dehydrogenase activity at end-stage (P150-175) was statistically significant by a Bonferroni multiple comparison post test (p<0.05, Fig 7).

Triheptanoin slightly increased plasma ketone (β-hydroxybutyrate) levels

Triheptanoin treated hSOD1^{G93A} mice showed a 56% increase in levels of plasma β-hydroxybutyrate compared to those treated with control diet (One-way ANOVA p = 0.042; p<0.05 Fisher's LSD post test, Fig 8). Similarly, triheptanoin also increased plasma β-hydroxybutyrate levels in wild-type mice by 96% (p = 0.0008, p<0.001) (Fig 8). However, in both wild-type and hSOD1^{G93A} mice following triheptanoin treatment, no differences were seen in plasma glucose levels, with average levels between 213–219 mg/dl (One-way ANOVA, p = 0.99).
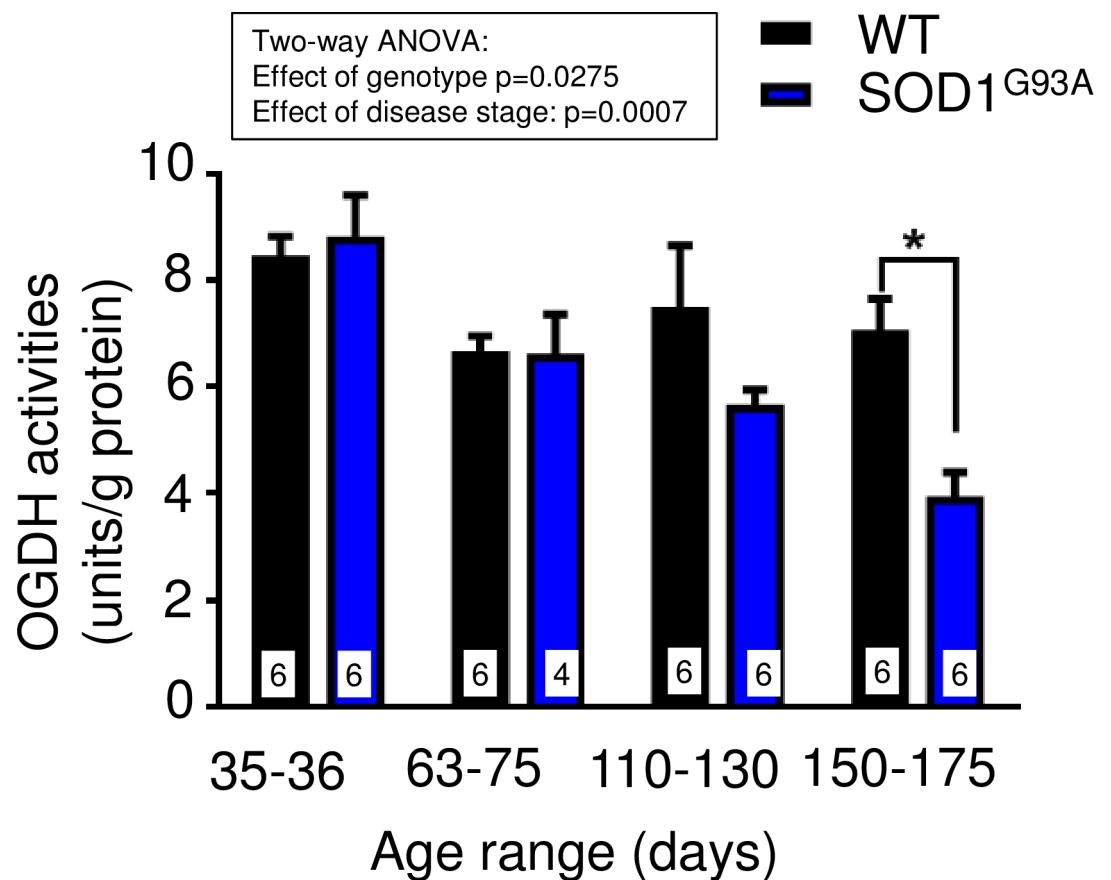

Fig 7. Lower maximal activities of 2-oxoglutarate dehydrogenase (OGDH) in hSOD1^{G93A} gastrocnemius muscle. The maximal activities of OGDH in extracts from gastrocnemius muscle of male wild-type and hSOD1^{G93A} mice at different disease stages are compared. Stages are defined as presymptomatic (days 35–36), onset (days 63–75), mid-stage (days 110–130) and end-stage (days 150–175). The inset above the graph shows the two-way ANOVA p-values for the effects of genotype and disease stage, indicating that 2-oxoglutarate activity in hSOD1^{G93A} mice declines with progression of disease. The star denotes significance in the Bonferroni post test (* p<0.05).
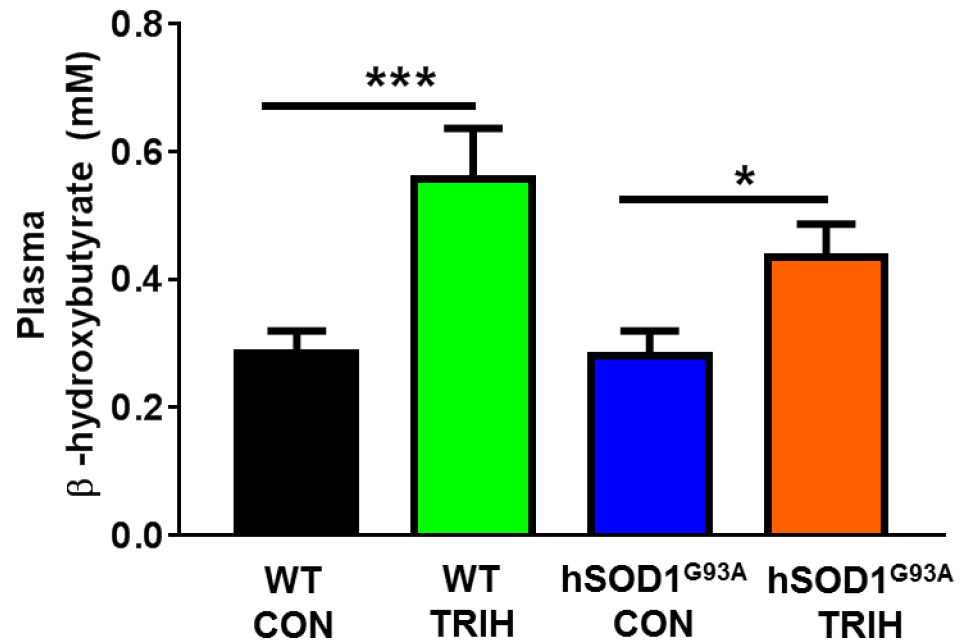
doi:10.1371/journal.pone.0161816.g007

Fig 8. Triheptanoin treatment increased levels of plasma β-hydroxybutyrate. Plasma β-hydroxybutyrate levels (mM) in 70 days old wild-type and hSOD1^{G93A} mice fed with either triheptanoin (TRIH) or control (CON) diet from day 35 to 70 (One-way ANOVA p = 0.042; Fisher's LSD post test: *p<0.05, ***p<0.001, n = 10–12).

doi:10.1371/journal.pone.0161816.g008

Discussion

The most important findings of this study are that 1) triheptanoin attenuated motor neuron loss in hSOD1^{G93A} mice, 2) triheptanoin delayed the onset of motor symptoms in hSOD1^{G93A} mice, and 3) decreased expression of muscle enzyme mRNA involved in TCA cycling in hSOD1^{G93A} mice was attenuated by triheptanoin. The hypothesized mechanisms by which triheptanoin protects motor neurons and delays muscle wasting is summarized in Fig 9.

Neuroprotective Effects of Triheptanoin

In our study, triheptanoin treated hSOD1^{G93A} mice showed 33% less motor neuron loss in the L4-L5 spinal cord. Similarly, in two other neurological disorders models the same dose of triheptanoin was found to protect cells. In *nur7* mutant mice, a model for Canavan disease, triheptanoin treatment prevented the loss of oligodendrocytes [65]. In a mouse middle cerebral artery occlusion (MCAO) model of stroke, triheptanoin pre-treatment reduced the infarct area and mitochondrial function was preserved in mitochondria isolated from brains 1 h after onset of MCAO [64]. Based on the previous findings that triheptanoin diminished abnormalities in brain energy metabolism in different models and patients with CNS disorders [55,56,59,60] it is likely that improvements in ATP production contribute to triheptanoin's neuroprotective effects. In addition, in an Alzheimer's Disease model, triheptanoin in the context of a ketogenic diet increased the expression of the mRNA levels of *Sirt1*, *Pparg*, *Sod1* and *Sod2* [75]. Sirtuin 1 and PPAR-γ are regulators of lipid and glucose metabolism as well as mitochondrial respiration and oxidative stress. Thus, these studies indicate that the neuroprotective effects of triheptanoin may be mediated, in part, by limiting oxidative stress and by preserving mitochondrial function, which together with triheptanoin's direct provision of alternative and anaplerotic fuel will contribute to improved energy supply.
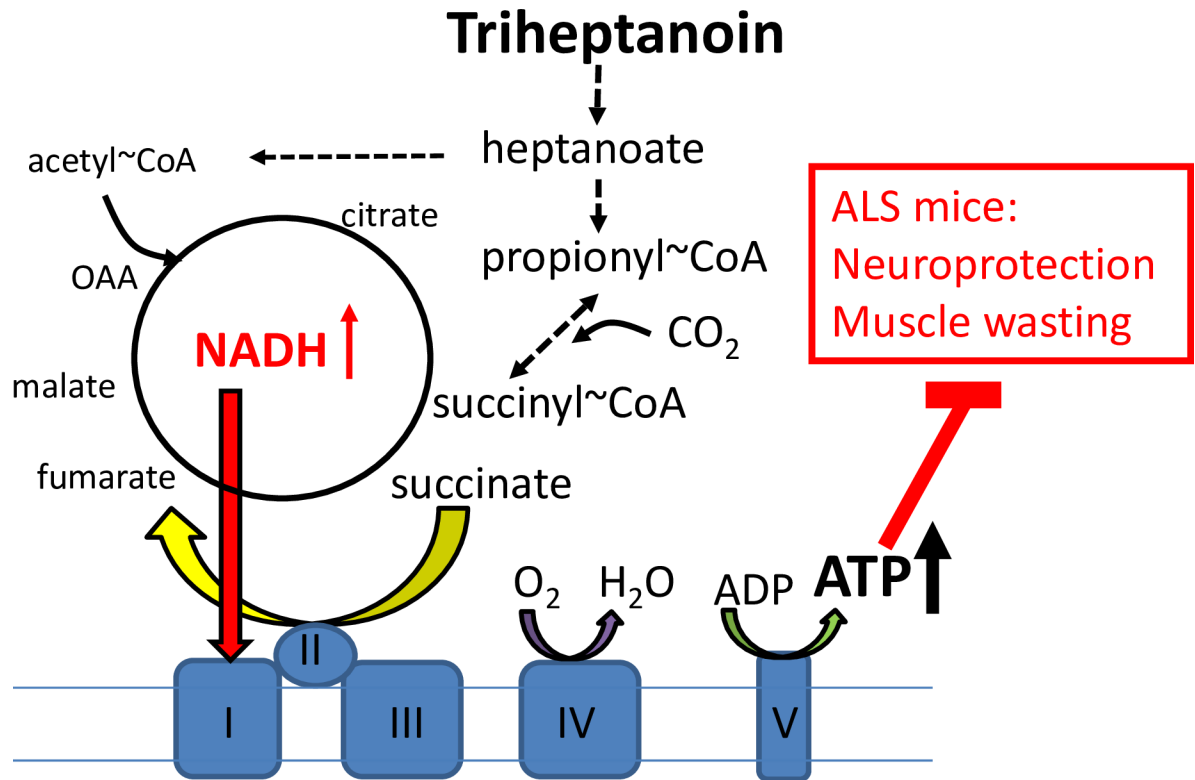
Fig 9. Hypothesized mechanisms of triheptanoin. Triheptanoin is the triglyceride of heptanoate, which is metabolized to acetyl-CoA as well as propionyl-CoA providing alternative and anaplerotic fuel. Following carboxylation propionyl-CoA produces succinyl-CoA (anaplerosis), which via metabolism to oxaloacetate can increase ATP production and aid in further acetyl-CoA oxidation. Thus triheptanoin can improve mitochondrial energy production and thereby protect neurons and muscle against degeneration.

doi:10.1371/journal.pone.0161816.g009

Clinical Importance of Triheptanoin's Protective Effects on ALS Symptoms

In addition to its neuroprotective effects, triheptanoin delayed the onset of the loss of grip strength by 2.8 weeks in hSOD1^{G93A} mice. This corresponds to 11% of the life span and 30% of the "symptomatic" time in these mice. Thus, our data show an improvement in disease symptoms when treatment was initiated prior to the onset of disease symptoms in hSOD1^{G93A} mice. This raises hope that in ALS patients, triheptanoin may be able to preserve motor neurons and the function of muscles when treatment is initiated at an early stage of disease.

On the other hand, presymptomatic hSOD1^{G93A} mice already show loss of crural flexor motor neurons [67]. This indicates that in ALS mouse models, pathological neuron loss does not necessarily translate to discernable motor deficits in mice, while motor deficits in patients may be present at a similar pathological stage. Thus, while triheptanoin was given at a presymptomatic stage of disease in mice, it is difficult to correlate our findings to the clinical course of disease in patients. Given the difficulty in diagnosing ALS, future studies are required to evaluate the extent to which triheptanoin can preserve motor neurons and motor function when treatment is initiated in ALS models with obvious muscle and/or neuronal impairments.

As a medium chain triglyceride, triheptanoin quickly provides heptanoic acid and C5 ketones to the blood. These molecules cross the blood brain barrier and are expected to also be metabolized by muscle. Therefore, it is anticipated that the protective effects of triheptanoin will begin quickly after the initiation of treatment. Because triheptanoin was safe in pilot

studies with patients with disorders involving severe metabolic deficiencies [54,76,77], CNS disorders [55,56,76], Pompe's Disease and Inclusion Body Myositis [57], there are relatively few hurdles to overcome to start a phase I clinical trial to assess safety and tolerability for patients with ALS. It will be important to rule out potential and known metabolic contraindications in study subjects and to provide professional dietary advice in addition to triheptanoin treatment. To date, no central or cardiovascular side effects have been reported for triheptanoin. For medium chain fats, the most common side effects consist of abdominal pain, diarrhea and nausea, which can largely be controlled by mixing the treatment with food and slowly increasing the dose. Given previous reports of gastric dysfunction in ALS patients [78,79], it is also pertinent that the impact of triheptanoin on gut function in ALS be investigated.

As a means to circumvent potential side effects of oral triheptanoin on gut function, triheptanoin could be delivered intravenously in an emulsion. This route of delivery would circumvent the known side effects on the GI tract and supply heptanoate quickly to various tissues before it reaches the liver. The liver can convert heptanoate to glucose via gluconeogenesis and thus reduces the amounts of heptanoate and C5 ketones that can reach other tissues. Such a triheptanoin emulsion is currently being developed by industry. Triheptanoin is an ideal precursor to supply heptanoic acid and C5 ketones to the body, although these metabolites should also be directly effective for patients. However, large amounts of heptanoic acid and C5 ketones or their sodium salts are unsuitable for direct application, as they would add unphysiological levels of acid or salt to the body.

It is now thought that the majority of clinical trials addressing the efficacy of new treatments in ALS have failed due to the lack of solid preclinical data. Consequently, new guidelines have been developed for laboratory work before phase II trials [73], including power analyses and high animal numbers when claiming effects on survival. While our power analyses regarding loss of grip strength and balance show that our study used adequate numbers of mice regarding these analyses of motor symptoms, a larger and more complete preclinical study of triheptanoin following the mentioned guidelines would be ideal to test its effect on survival in multiple animal models of ALS. Also, treatment initiation during the symptomatic stage and assessments of muscle function and the integrity of neuromuscular junctions will be important to inform and motivate clinical trials.

Metabolic Changes in hSOD1^{G93A} Mouse Muscle

When compared to healthy wild-type mice, we found that the expression of several enzyme mRNA involved in glycolysis, the TCA cycle and anaplerosis were significantly reduced in the gastrocnemius muscle of hSOD1^{G93A} mice at 10 weeks of age (Figs 4–6), a time when hind limb grip strength is still normal (Fig 3B). We also demonstrate that the maximal 2-oxoglutarate dehydrogenase activity was significantly reduced based on genotype and disease stage in gastrocnemius muscle in hSOD1^{G93A} compared to wild-type mice (Fig 7), indicating that the observed mRNA changes result in functional alterations. Taken together this suggests that ATP production is insufficient in the muscle for the function and maintenance of tissue at an early stage of the disease. Similar changes in mRNA levels were seen at the end-stage of disease at 25 weeks of age (Figs 4–6), highlighting that an impairment of TCA cycling may persist throughout the progression of disease.

Numerous studies have alluded to altered energy metabolism during the early and later stages of disease progression in muscle in ALS patients and in ALS mouse models [25,29–33,35]. In the majority of sporadic ALS patients, respiratory chain defects and multiple deletions in mitochondrial DNA have been observed in muscle biopsies [24], suggesting that metabolic abnormalities occur in muscle and that muscle pathology may contribute to ALS.

Moreover, citrate synthase activity was decreased by 43% in muscle from ALS patients when compared to healthy controls [32]. Consistent with this, ALS patients displayed increased blood lactate levels, especially after exercise, indicating that acetyl-CoA is not metabolized well by the TCA cycle [80]. Furthermore, SOD1 mouse models of ALS showed reduced levels of ATP in skeletal muscle [35,36]. Moreover, oxidative stress, which is commonly observed in ALS (reviewed in [12,81]), is well known to diminish the activities of CNS and muscle aconitase and 2-oxoglutarate dehydrogenase, both enzymes of the TCA cycle [82,83].

At 25 weeks, we found reduced levels of the main anaplerotic enzyme mRNA of muscle, glutamic pyruvic transaminase 2, suggesting diminished levels of TCA cycle intermediates. Triheptanoin prevented the downregulation of several enzyme mRNA observed in hSOD1^{G93A} when compared to wild-type mice. This finding implies that normalization of energy metabolism by triheptanoin prevents downregulation of certain metabolism genes, which in turn would help to maintain a healthy metabolism to optimize energy supply, function and survival of tissue. When considering these collective metabolic alterations, it is not surprising that triheptanoin, which is currently the most effective treatment to produce anaplerotic propionyl-CoA slowed the onset of motor symptoms in hSOD1^{G93A} mice.

Triheptanoin and Body Weight

Loss of body weight is a concern in many ALS patients and is an indicator for ALS progression during the later stages of disease in the hSOD1^{G93A} mouse. In this study, triheptanoin slowed body weight increases in the wild-type C57BL/6 mice. This effect has been previously mentioned for medium chain triglycerides, which in contrast to long chain fats, do not accumulate in adipose tissue (reviewed by [84]). However, in patients with muscular and neurological disorders, treatment with triheptanoin has not been reported to induce a loss in body weight. Rather increases in weight were seen in some patients [57]. Also, mice from two outbred strains gained weight equally with and without triheptanoin treatment [63,66]. In spite of a trend to lower body weight in this study, mice on triheptanoin showed similar hind limb grip strength when compared to untreated mice, indicating that lower body weight does not impair muscle function. In addition, despite this potential confounding factor, triheptanoin treated mice showed a delay in the loss of body weight and similar survival when compared to untreated mice. If triheptanoin treatment is tested in ALS models on background strains that do not exhibit a loss in body weight, it is likely that the disease modifying effects of triheptanoin will be further enhanced, potentially improving survival.

Comparison to Other Metabolic Treatment Approaches for ALS

Other metabolic treatment approaches have been tested in hSOD1^{G93A} mice. Ketogenic therapy, which increases blood C4 ketone levels is commonly thought to improve the production of ATP by mitochondria [85]. When tested in hSOD1^{G93A} mice, a ketogenic diet preserved motor performance and delayed weight loss and loss of motor neurons in the lumbar spinal cord [86]. Similarly, trioctanoin (caprylic triglyceride, the triglyceride of octanoate), which also increases blood C4 ketone levels, increased oxygen consumption rates in mitochondria of the spinal cord, delayed onset of motor symptoms and protected motor neurons [87]. However, both treatments did not extend survival in hSOD1^{G93A} mice and ketogenic therapy is contraindicated in ALS as it typically leads to weight loss in adults. Our recent study indicated that chronic trioctanoin, but not triheptanoin, treatment can decrease glycolysis and the levels of TCA cycle intermediates in mouse brain tissue [88]. Thus, trioctanoin treatment alone might interfere with the generation of energy from glucose, which may worsen metabolic problems in ALS (reviewed in [89]). In the same study triheptanoin feeding to CD1 mice increased brain β-

hydroxybutyrate levels 1.7-fold, which may contribute to its beneficial effects. Similarly, in the current study plasma levels of the C4 ketone β-hydroxybutyrate were increased with triheptanoin treatment in hSOD1^{G93A} mice by 1.6-fold (Fig 8). In addition, triheptanoin is expected to be superior to any fuel that produces C4 ketones, because triheptanoin is anaplerotic.

Dichloroacetate, a metabolic treatment that increases pyruvate dehydrogenase activity, has been found to improve survival time and/or delay the loss of motor function in SOD1 mice [49,90]. An increase in pyruvate dehydrogenase kinase activity is expected to allow more efficient production of energy from glucose, if there is sufficient TCA cycling. However, studies are needed to determine the impact of dichloroacetate on TCA cycle metabolism in order to allow a better understanding of this potential treatment approach in ALS.

There is evidence that some ALS patients benefitted from the "Deanna Protocol", a complex combination of many metabolic supplements, in addition to medium chain triglyceride-rich coconut oil [91]. More recently, [92] showed the beneficial effects of a simplified "Deanna Protocol" in hSOD1^{G93A} mice. Specifically, a combination of arginine α-ketoglutarate, β-phenyl-γ-amino butyrate, ubiquinone and medium even chain triglyceride oil, which is largely a mixture of triglycerides of octanoate and decanoate, extended survival. Providing that α-ketoglutarate or a C5 or C4 metabolite of this compound enters mitochondria, the TCA cycle metabolite pool could be (re-)filled and this treatment can be considered as being "anaplerotic" similar to heptanoate. This would aid the metabolism of the co-supplied alternative medium chain fatty acids, octanoate and decanoate, which taken together closely resembles the proposed mechanism of action of triheptanoin. Despite current reports of beneficial outcomes in response to dietary intervention strategies in mouse models of ALS, the extent to which dichloroacetate, the Deanna protocol and triheptanoin are efficacious in controlled clinical trials remains to be investigated.

Conclusion

This study revealed that triheptanoin is a promising new treatment approach for ALS to delay motor neuron loss and the onset of motor symptoms. Further studies with increased animal numbers and treatment initiation in symptomatic stages, and those that use ^{13}C-labeled glucose or heptanoate are necessary to elucidate triheptanoin's metabolic fate and mechanism of action in ALS. Such studies will be important to inform and optimize future clinical trials.

Acknowledgments

Author Contributions

Conceptualization: KB STN.

Data curation: TWT YW MEB NKT TSM.

Formal analysis: TWT YW KB.

Funding acquisition: KB.

Investigation: TWT YW MEB NKT TSM.

Methodology: STN TSM.

Project administration: KB.

Resources: KB.

Supervision: KB.

Validation: TWT KB.

Visualization: TWT YW MEB KB.

Writing – original draft: TWT YW.

Writing – review & editing: TWT YW MEB NKT STN TSM KB.

References

1. Baumer D, Talbot K, Turner MR (2014) Advances in motor neurone disease. Journal of the Royal Society of Medicine 107: 14–21. doi: 10.1177/0141076813511451 PMID: 24399773

2. Cleveland DW, Rothstein JD (2001) From Charcot to Lou Gehrig: deciphering selective motor neuron death in ALS. Nature reviews Neuroscience 2: 806–819. PMID: 11715057

3. Chen S, Sayana P, Zhang X, Le W (2013) Genetics of amyotrophic lateral sclerosis: an update. Molecular neurodegeneration 8: 28. doi: 10.1186/1750-1326-8-28 PMID: 23941283

4. Rosen DR, Siddique T, Patterson D, Figlewicz DA, Sapp P, Hentati A, et al. (1993) Mutations in Cu/Zn superoxide dismutase gene are associated with familial amyotrophic lateral sclerosis. Nature 362: 59–62. PMID: 8446170

5. Kabashi E, Valdmanis PN, Dion P, Spiegelman D, McConkey BJ, Vande Velde C, et al. (2008) TARDBP mutations in individuals with sporadic and familial amyotrophic lateral sclerosis. Nature genetics 40: 572–574. doi: 10.1038/ng.132 PMID: 18372902

6. Kwiatkowski TJ Jr., Bosco DA, Leclerc AL, Tamrazian, Vanderburg CR, Russ C, et al. (2009) Mutations in the FUS/TLS gene on chromosome 16 cause familial amyotrophic lateral sclerosis. Science 323: 1205–1208. doi: 10.1126/science.1166066 PMID: 19251627

7. Deng HX, Chen W, Hong ST, Boycott KM, Gorrie GH, Siddique N, et al. (2011) Mutations in UBQLN2 cause dominant X-linked juvenile and adult-onset ALS and ALS/dementia. Nature 477: 211–215. doi: 10.1038/nature10353 PMID: 21857683

8. DeJesus-Hernandez M, Mackenzie IR, Boeve BF, Boxer AL, Baker M, Rutherford NJ, et al. (2011) Expanded GGGGCC hexanucleotide repeat in noncoding region of C9ORF72 causes chromosome 9p-linked FTD and ALS. Neuron 72: 245–256. doi: 10.1016/j.neuron.2011.09.011 PMID: 21944778

9. Renton AE, Majounie E, Waite A, Simon-Sanchez J, Rollinson S, Gibbs JR, et al. (2011) A hexanucleotide repeat expansion in C9ORF72 is the cause of chromosome 9p21-linked ALS-FTD. Neuron 72: 257–268. doi: 10.1016/j.neuron.2011.09.010 PMID: 21944779

10. Kiernan MC, Vucic S, Cheah BC, Turner MR, Eisen A, Hardiman O, et al. (2011) Amyotrophic lateral sclerosis. Lancet 377: 942–955. doi: 10.1016/S0140-6736(10)61156-7 PMID: 21296405

11. Milani P, Gagliardi S, Cova E, Cereda C (2011) SOD1 Transcriptional and Posttranscriptional Regulation and Its Potential Implications in ALS. Neurol Res Int 2011: 458427. doi: 10.1155/2011/458427 PMID: 21603028

12. Cozzolino M, Carri MT (2012) Mitochondrial dysfunction in ALS. Prog Neurobiol 97: 54–66. doi: 10.1016/j.pneurobio.2011.06.003 PMID: 21827820

13. Turner BJ, Talbot K (2008) Transgenics, toxicity and therapeutics in rodent models of mutant SOD1-mediated familial ALS. Prog Neurobiol 85: 94–134. doi: 10.1016/j.pneurobio.2008.01.001 PMID: 18282652

14. Vucic S, Kiernan MC (2009) Pathophysiology of neurodegeneration in familial amyotrophic lateral sclerosis. Curr Mol Med 9: 255–272. PMID: 19355908

15. Shi P, Wei Y, Zhang J, Gal J, Zhu H (2010) Mitochondrial dysfunction is a converging point of multiple pathological pathways in amyotrophic lateral sclerosis. J Alzheimers Dis 20 Suppl 2: S311–324. doi: 10.3233/JAD-2010-100366 PMID: 20463400

16. Ferraiuolo L, Kirby J, Grierson AJ, Sendtner M, Shaw PJ (2011) Molecular pathways of motor neuron injury in amyotrophic lateral sclerosis. Nature reviews Neurology 7: 616–630. doi: 10.1038/nrneurol.2011.152 PMID: 22051914

17. Barber SC, Mead RJ, Shaw PJ (2006) Oxidative stress in ALS: a mechanism of neurodegeneration and a therapeutic target. Biochimica et biophysica acta 1762: 1051–1067. PMID: 16713195

18. Rothstein JD, Tsai G, Kuncl RW, Clawson L, Cornblath DR, Drachman DB, et al. (1990) Abnormal excitatory amino acid metabolism in amyotrophic lateral sclerosis. Annals of neurology 28: 18–25. PMID: 2375630

19. McGeer PL, McGeer EG (2002) Inflammatory processes in amyotrophic lateral sclerosis. Muscle & nerve 26: 459–470.

20. Bruijn LI, Houseweart MK, Kato S, Anderson KL, Anderson SD, Ohama E, et al. (1998) Aggregation and motor neuron toxicity of an ALS-linked SOD1 mutant independent from wild-type SOD1. Science 281: 1851–1854. PMID: 9743498

21. Julien JP, Beaulieu JM (2000) Cytoskeletal abnormalities in amyotrophic lateral sclerosis: beneficial or detrimental effects? Journal of the neurological sciences 180: 7–14. PMID: 11090858

22. Dupuis L, Oudart H, Rene F, Gonzalez de Aguilar JL, Loeffler JP (2004) Evidence for defective energy homeostasis in amyotrophic lateral sclerosis: benefit of a high-energy diet in a transgenic mouse model. Proceedings of the National Academy of Sciences of the United States of America 101: 11159–11164. PMID: 15263088

23. Dupuis L, Pradat PF, Ludolph AC, Loeffler JP (2011) Energy metabolism in amyotrophic lateral sclerosis. The Lancet Neurology 10: 75–82. doi: 10.1016/S1474-4422(10)70224-6 PMID: 21035400

24. Vielhaber S, Kunz D, Winkler K, Wiedemann FR, Kirches E, Feistner H, et al. (2000) Mitochondrial DNA abnormalities in skeletal muscle of patients with sporadic amyotrophic lateral sclerosis. Brain 123 (Pt 7): 1339–1348. PMID: 10869047

25. Crugnola V, Lamperti C, Lucchini V, Ronchi D, Peverelli L, Prelle A, et al. (2010) Mitochondrial respiratory chain dysfunction in muscle from patients with amyotrophic lateral sclerosis. Archives of neurology 67: 849–854. doi: 10.1001/archneurol.2010.128 PMID: 20625092

26. Kong J, Xu Z (1998) Massive mitochondrial degeneration in motor neurons triggers the onset of amyotrophic lateral sclerosis in mice expressing a mutant SOD1. Journal of Neuroscience 18: 3241–3250. PMID: 9547233

27. Sasaki S, Iwata M (1996) Ultrastructural study of synapses in the anterior horn neurons of patients with amyotrophic lateral sclerosis. Neuroscience letters 204: 53–56. PMID: 8929976

28. Wong PC, Pardo CA, Borchelt DR, Lee MK, Copeland NG, Jenkins NA, et al. (1995) An adverse property of a familial ALS-linked SOD1 mutation causes motor neuron disease characterized by vacuolar degeneration of mitochondria. Neuron 14: 1105–1116. PMID: 7605627

29. Vielhaber S, Winkler K, Kirches E, Kunz D, Buchner M, Feistner H, et al. (1999) Visualization of defective mitochondrial function in skeletal muscle fibers of patients with sporadic amyotrophic lateral sclerosis. Journal of the neurological sciences 169: 133–139. PMID: 10540022

30. Wiedemann FR, Winkler K, Kuznetsov AV, Bartels C, Vielhaber S, Feistner H, et al. (1998) Impairment of mitochondrial function in skeletal muscle of patients with amyotrophic lateral sclerosis. Journal of the neurological sciences 156: 65–72. PMID: 9559989

31. Luo G, Yi J, Ma C, Xiao Y, Yi F, Yu T, et al. (2013) Defective mitochondrial dynamics is an early event in skeletal muscle of an amyotrophic lateral sclerosis mouse model. PloS one 8: e82112. doi: 10.1371/journal.pone.0082112 PMID: 24324755

32. Russell AP, Wada S, Vergani L, Hock MB, Lamon S, Leger B, et al. (2013) Disruption of skeletal muscle mitochondrial network genes and miRNAs in amyotrophic lateral sclerosis. Neurobiology of disease 49: 107–117. doi: 10.1016/j.nbd.2012.08.015 PMID: 22975021

33. Echaniz-Laguna A, Zoll J, Ponsot E, N'Guessan B, Tranchant C, Loeffler JP, et al. (2006) Muscular mitochondrial function in amyotrophic lateral sclerosis is progressively altered as the disease develops: a temporal study in man. Experimental neurology 198: 25–30. PMID: 16126198

34. Mattiazzi M, D'Aurelio M, Gajewski CD, Martushova K, Kiaei M, Beal MF, et al. (2002) Mutated human SOD1 causes dysfunction of oxidative phosphorylation in mitochondria of transgenic mice. The Journal of biological chemistry 277: 29626–29633. PMID: 12050154

35. Dupuis L, di Scala F, Rene F, de Tapia M, Oudart H, Pradat PF, et al. (2003) Up-regulation of mitochondrial uncoupling protein 3 reveals an early muscular metabolic defect in amyotrophic lateral sclerosis. FASEB J 17: 2091–2093. PMID: 14500553

36. Derave W, Van Den Bosch L, Lemmens G, Eijnde BO, Robberecht W, Hespel P (2003) Skeletal muscle properties in a transgenic mouse model for amyotrophic lateral sclerosis: effects of creatine treatment. Neurobiology of disease 13: 264–272. PMID: 12901841

37. Browne SE, Bowling AC, Baik MJ, Gurney M, Brown RH Jr, Beal MF (1998) Metabolic dysfunction in familial, but not sporadic, amyotrophic lateral sclerosis. Journal of neurochemistry 71: 281–287. PMID: 9648876

38. Dalakas MC, Hatazawa J, Brooks RA, Di Chiro G (1987) Lowered cerebral glucose utilization in amyotrophic lateral sclerosis. Annals of neurology 22: 580–586. PMID: 3501273

39. Hatazawa J, Brooks RA, Dalakas MC, Mansi L, Di Chiro G (1988) Cortical motor-sensory hypometabolism in amyotrophic lateral sclerosis: a PET study. Journal of computer assisted tomography 12: 630–636. PMID: 3260610

40. Ludolph AC, Langen KJ, Regard M, Herzog H, Kemper B, Kuwert T, et al. (1992) Frontal lobe function in amyotrophic lateral sclerosis: a neuropsychologic and positron emission tomography study. Acta neurologica Scandinavica 85: 81–89. PMID: 1574993

41. Cistaro A, Valentini MC, Chio A, Nobili F, Calvo A, Moglia C, et al. (2012) Brain hypermetabolism in amyotrophic lateral sclerosis: a FDG PET study in ALS of spinal and bulbar onset. European journal of nuclear medicine and molecular imaging 39: 251–259. doi: 10.1007/s00259-011-1979-6 PMID: 22089661

42. Pagani M, Chio A, Valentini MC, Oberg J, Nobili F, Calvo A, et al. (2014) Functional pattern of brain FDG-PET in amyotrophic lateral sclerosis. Neurology 83: 1067–1074. doi: 10.1212/WNL.0000000000000792 PMID: 25122207

43. Miyazaki K, Masamoto K, Morimoto N, Kurata T, Mimoto T, Obata T, et al. (2012) Early and progressive impairment of spinal blood flow-glucose metabolism coupling in motor neuron degeneration of ALS model mice. Journal of cerebral blood flow and metabolism: official journal of the International Society of Cerebral Blood Flow and Metabolism 32: 456–467.

44. Smittkamp SE, Morris JK, Bomhoff GL, Chertoff ME, Geiger PC, Stanford JA (2014) SOD1-G93A mice exhibit muscle-fiber-type-specific decreases in glucose uptake in the absence of whole-body changes in metabolism. Neuro-degenerative diseases 13: 29–37. doi: 10.1159/000351606 PMID: 24021858

45. Raman R, Allen SP, Goodall EF, Kramer S, Ponger LL, Heath PR, et al. (2015) Gene expression signatures in motor neurone disease fibroblasts reveal dysregulation of metabolism, hypoxia-response and RNA processing functions. Neuropathology and applied neurobiology 41: 201–226. doi: 10.1111/nan.12147 PMID: 24750211

46. Lederer CW, Torrisi A, Pantelidou M, Santama N, Cavallaro S (2007) Pathways and genes differentially expressed in the motor cortex of patients with sporadic amyotrophic lateral sclerosis. BMC genomics 8: 26. PMID: 17244347

47. Wang XS, Simmons Z, Liu W, Boyer PJ, Connor JR (2006) Differential expression of genes in amyotrophic lateral sclerosis revealed by profiling the post mortem cortex. Amyotrophic lateral sclerosis: official publication of the World Federation of Neurology Research Group on Motor Neuron Diseases 7: 201–210.

48. Saris CG, Groen EJ, van Vught PW, van Es MA, Blauw HM, Veldink JH, et al. (2013) Gene expression profile of SOD1-G93A mouse spinal cord, blood and muscle. Amyotrophic lateral sclerosis & frontotemporal degeneration 14: 190–198.

49. Palamiuc L, Schlagowski A, Ngo ST, Vernay A, Dirrig-Grosch S, Henriques A, et al. (2015) A metabolic switch toward lipid use in glycolytic muscle is an early pathologic event in a mouse model of amyotrophic lateral sclerosis. EMBO Mol Med 7: 526–546. doi: 10.15252/emmm.201404433 PMID: 25820275

50. Choi JK, Kustermann E, Dedeoglu A, Jenkins BG (2009) Magnetic resonance spectroscopy of regional brain metabolite markers in FALS mice and the effects of dietary creatine supplementation. The European journal of neuroscience 30: 2143–2150. doi: 10.1111/j.1460-9568.2009.07015.x PMID: 19930399

51. Niessen HG, Debska-Vielhaber G, Sander K, Angenstein F, Ludolph AC, Hilfert L, et al. (2007) Metabolic progression markers of neurodegeneration in the transgenic G93A-SOD1 mouse model of amyotrophic lateral sclerosis. Eur J Neurosci 25: 1669–1677. PMID: 17432958

52. D'Alessandro G, Calcagno E, Tartari S, Rizzardini M, Invernizzi RW, Cantoni L (2011) Glutamate and glutathione interplay in a motor neuronal model of amyotrophic lateral sclerosis reveals altered energy metabolism. Neurobiol Dis 43: 346–355. doi: 10.1016/j.nbd.2011.04.003 PMID: 21530659

53. Brunengraber H, Roe CR (2006) Anaplerotic molecules: Current and future. J Inherit Metab Dis 29: 327–331. PMID: 16763895

54. Roe CR, Mochel F (2006) Anaplerotic diet therapy in inherited metabolic disease: Therapeutic potential. J Inherit Metab Dis 29: 332–340. PMID: 16763896

55. Adanyeguh IM, Rinaldi D, Henry PG, Caillet S, Valabregue R, Durr A, et al. (2015) Triheptanoin improves brain energy metabolism in patients with Huntington disease. Neurology 84: 490–495. doi: 10.1212/WNL.0000000000001214 PMID: 25568297

56. Pascual JM, Liu P, Mao D, Kelly DI, Hernandez A, Sheng M, et al. (2014) Triheptanoin for glucose transporter type I deficiency (G1D): modulation of human ictogenesis, cerebral metabolic rate, and cognitive indices by a food supplement. JAMA Neurol 71: 1255–1265. doi: 10.1001/jamaneurol.2014.1584 PMID: 25110966

57. Corbett A, Garg N, Crosbie A, Borges K (2015) A Pilot Study of Triheptanoin Treatment in Sporadic Inclusion Body Myositis (sIBM). Annals of Neurology 78: S102.

58. Gu L, Zhang GF, Kombu RS, Allen F, Kutz G, Brewer WU, et al. (2010) Parenteral and enteral metabolism of anaplerotic triheptanoin in normal rats. II. Effects on lipolysis, glucose production, and liver acyl-

CoA profile. Am J Physiol Endocrinol Metab 298: E362–371. doi: 10.1152/ajpendo.00384.2009 PMID: 19903863

59. Marin-Valencia I, Good LB, Ma Q, Malloy CR, Pascual JM (2013) Heptanoate as a neural fuel: energetic and neurotransmitter precursors in normal and glucose transporter I-deficient (G1D) brain. J Cereb Blood Flow Metab 33: 175–182. doi: 10.1038/jcbfm.2012.151 PMID: 23072752

60. Hadera MG, Smeland OB, McDonald TS, Tan KN, Sonnewald U, Borges K (2014) Triheptanoin partially restores levels of tricarboxylic acid cycle intermediates in the mouse pilocarpine model of epilepsy. J Neurochem 129: 107–119. doi: 10.1111/jnc.12610 PMID: 24236946

61. Borges K, Sonnewald U (2012) Triheptanoin—a medium chain triglyceride with odd chain fatty acids: a new anaplerotic anticonvulsant treatment? Epilepsy Res 100: 239–244. doi: 10.1016/j.eplepsyres.2011.05.023 PMID: 21855298

62. Mochel F, Duteil S, Marelli C, Jauffret C, Barles A, Holm J, et al. (2010) Dietary anaplerotic therapy improves peripheral tissue energy metabolism in patients with Huntington's disease. Eur J Hum Genet 18: 1057–1060. doi: 10.1038/ejhg.2010.72 PMID: 20512158

63. Willis S, Stoll J, Sweetman L, Borges K (2010) Anticonvulsant effects of a triheptanoin diet in two mouse chronic seizure models. Neurobiol Dis 40: 565–572. doi: 10.1016/j.nbd.2010.07.017 PMID: 20691264

64. Schwarzkopf TM, Koch K, Klein J (2015) Reduced severity of ischemic stroke and improvement of mitochondrial function after dietary treatment with the anaplerotic substance triheptanoin. Neuroscience 300: 201–209. doi: 10.1016/j.neuroscience.2015.05.014 PMID: 25982559

65. Francis JS, Markov V, Leone P (2014) Dietary triheptanoin rescues oligodendrocyte loss, dysmyelination and motor function in the nur7 mouse model of Canavan disease. J Inherit Metab Dis 37: 369–381. doi: 10.1007/s10545-013-9663-6 PMID: 24288037

66. Thomas NK, Willis S, Sweetman L, Borges K (2012) Triheptanoin in acute mouse seizure models. Epilepsy Res 99: 312–317. doi: 10.1016/j.eplepsyres.2011.12.013 PMID: 22260920

67. Ngo ST, Baumann F, Ridall PG, Pettitt AN, Henderson RD, Bellingham MC, et al. (2012) The relationship between Bayesian motor unit number estimation and histological measurements of motor neurons in wild-type and SOD1(G93A) mice. Clin Neurophysiol 123: 2080–2091. doi: 10.1016/j.clinph.2012.01.028 PMID: 22521362

68. Coggeshall RE, Lekan HA (1996) Methods for determining numbers of cells and synapses: a case for more uniform standards of review. J Comp Neurol 364: 6–15. PMID: 8789272

69. Gill A, Kidd J, Vieira F, Thompson K, Perrin S (2009) No benefit from chronic lithium dosing in a sibling-matched, gender balanced, investigator-blinded trial using a standard mouse model of familial ALS. PLoS One 4: e6489. doi: 10.1371/journal.pone.0006489 PMID: 19649300

70. Lee JD, Kamaruzaman NA, Fung JN, Taylor SM, Turner BJ, Atkin JD, et al. (2013) Dysregulation of the complement cascade in the hSOD1G93A transgenic mouse model of amyotrophic lateral sclerosis. J Neuroinflammation 10: 119. doi: 10.1186/1742-2094-10-119 PMID: 24067070

71. Vandesompele J, De Preter K, Pattyn F, Poppe B, Van Roy N, De Paepe A, et al. (2002) Accurate normalization of real-time quantitative RT-PCR data by geometric averaging of multiple internal control genes. Genome Biol 3: RESEARCH0034. PMID: 12184808

72. Lai JCK, Cooper AJL (1986) Brain α-Ketoglutarate Dehydrogenase Complex: Kinetic Properties, Regional Distribution, and Effects of Inhibitors. J Neurochem 47: 1376–1386. PMID: 3760866

73. Ludolph AC, Bendotti C, Blaugrund E, Chio A, Greensmith L, Loeffler JP, et al. (2010) Guidelines for preclinical animal research in ALS/MND: A consensus meeting. Amyotroph Lateral Scler 11: 38–45. doi: 10.3109/17482960903545334 PMID: 20184514

74. Steyn FJ, Ngo ST, Lee JD, Leong JW, Buckley AJ, Veldhuis JD, et al. (2012) Impairments to the GH-IGF-I axis in hSOD1G93A mice give insight into possible mechanisms of GH dysregulation in patients with amyotrophic lateral sclerosis. Endocrinology 153: 3735–3746. doi: 10.1210/en.2011-2171 PMID: 22621959

75. Aso E, Semakova J, Joda L, Semak V, Halbaut L, Calpena A, et al. (2013) Triheptanoin supplementation to ketogenic diet curbs cognitive impairment in APP/PS1 mice used as a model of familial Alzheimer's disease. Curr Alzheimer Res 10: 290–297. PMID: 23131121

76. Roe CR, Bottiglieri T, Wallace M, Arning E, Martin A (2010) Adult Polyglucosan Body Disease (APBD): Anaplerotic diet therapy (Triheptanoin) and demonstration of defective methylation pathways. Mol Genet Metab 101: 246–252. doi: 10.1016/j.ymgme.2010.06.017 PMID: 20655781

77. Roe CR, Yang BZ, Brunengraber H, Roe DS, Wallace M, Garritson BK (2008) Carnitine palmitoyltransferase II deficiency: successful anaplerotic diet therapy. Neurology 71: 260–264. doi: 10.1212/01.wnl.0000318283.42961.e9 PMID: 18645163

78. Camilleri M, Balm RK, Low PA (1993) Autonomic dysfunction in patients with chronic intestinal pseudo-obstruction. Clin Auton Res 3: 95–100. PMID: 8324379

79. Toepfer M, Folwaczny C, Klauser A, Riepl RL, Muller-Felber W, Pongratz D (1999) Gastrointestinal dysfunction in amyotrophic lateral sclerosis. Amyotroph Lateral Scler Other Motor Neuron Disord 1: 15–19. PMID: 12365061

80. Vadakkadath Meethal S, Atwood CS (2012) Lactate dyscrasia: a novel explanation for amyotrophic lateral sclerosis. Neurobiol Aging 33: 569–581. doi: 10.1016/j.neurobiolaging.2010.04.012 PMID: 20541840

81. Barber SC, Shaw PJ (2010) Oxidative stress in ALS: key role in motor neuron injury and therapeutic target. Free Radic Biol Med 48: 629–641. doi: 10.1016/j.freeradbiomed.2009.11.018 PMID: 19969067

82. Andersson U, Leighton B, Young ME, Blomstrand E, Newsholme EA (1998) Inactivation of aconitase and oxoglutarate dehydrogenase in skeletal muscle in vitro by superoxide anions and/or nitric oxide. Biochem Biophys Res Commun 249: 512–516. PMID: 9712727

83. Tretter L, Adam-Vizi V (2000) Inhibition of Krebs cycle enzymes by hydrogen peroxide: A key role of [alpha]-ketoglutarate dehydrogenase in limiting NADH production under oxidative stress. J Neurosci 20: 8972–8979. PMID: 11124972

84. Bach AC, Babayan VK (1982) Medium-chain triglycerides: an update. Am J Clin Nutr 36: 950–962. PMID: 6814231

85. Bough KJ, Rho JM (2007) Anticonvulsant mechanisms of the ketogenic diet. Epilepsia 48: 43–58. PMID: 17241207

86. Zhao Z, Lange DJ, Voustianiouk A, MacGrogan D, Ho L, Suh J, et al. (2006) A ketogenic diet as a potential novel therapeutic intervention in amyotrophic lateral sclerosis. BMC neuroscience 7: 29. PMID: 16584562

87. Zhao W, Varghese M, Vempati P, Dzhun A, Cheng A, Wang J, et al. (2012) Caprylic triglyceride as a novel therapeutic approach to effectively improve the performance and attenuate the symptoms due to the motor neuron loss in ALS disease. PloS one 7: e49191. doi: 10.1371/journal.pone.0049191 PMID: 23145119

88. McDonald TS, Tan KN, Hodson MP, Borges K (2014) Alterations of hippocampal glucose metabolism by even versus uneven medium chain triglycerides. J Cereb Blood Flow Metab 34: 153–160. doi: 10.1038/jcbfm.2013.184 PMID: 24169853

89. Ngo ST, Steyn FJ (2015) The interplay between metabolic homeostasis and neurodegeneration: insights into the neurometabolic nature of amyotrophic lateral sclerosis. Cell Regen (Lond) 4: 5.

90. Miquel E, Cassina A, Martinez-Palma L, Bolatto C, Trias E, Gandelman M, et al. (2012) Modulation of astrocytic mitochondrial function by dichloroacetate improves survival and motor performance in inherited amyotrophic lateral sclerosis. PloS one 7: e34776. doi: 10.1371/journal.pone.0034776 PMID: 22509356

91. ALS Untangled Group (2013) ALS Untangled No. 20: the Deanna protocol. Amyotroph Lateral Scler Frontotemporal Degener 14: 319–323. doi: 10.3109/21678421.2013.788405 PMID: 23638638

92. Ari C, Poff AM, Held HE, Landon CS, Goldhagen CR, Mavromates N, et al. (2014) Metabolic therapy with Deanna Protocol supplementation delays disease progression and extends survival in amyotrophic lateral sclerosis (ALS) mouse model. PLoS One 9: e103526. doi: 10.1371/journal.pone.0103526 PMID: 25061944